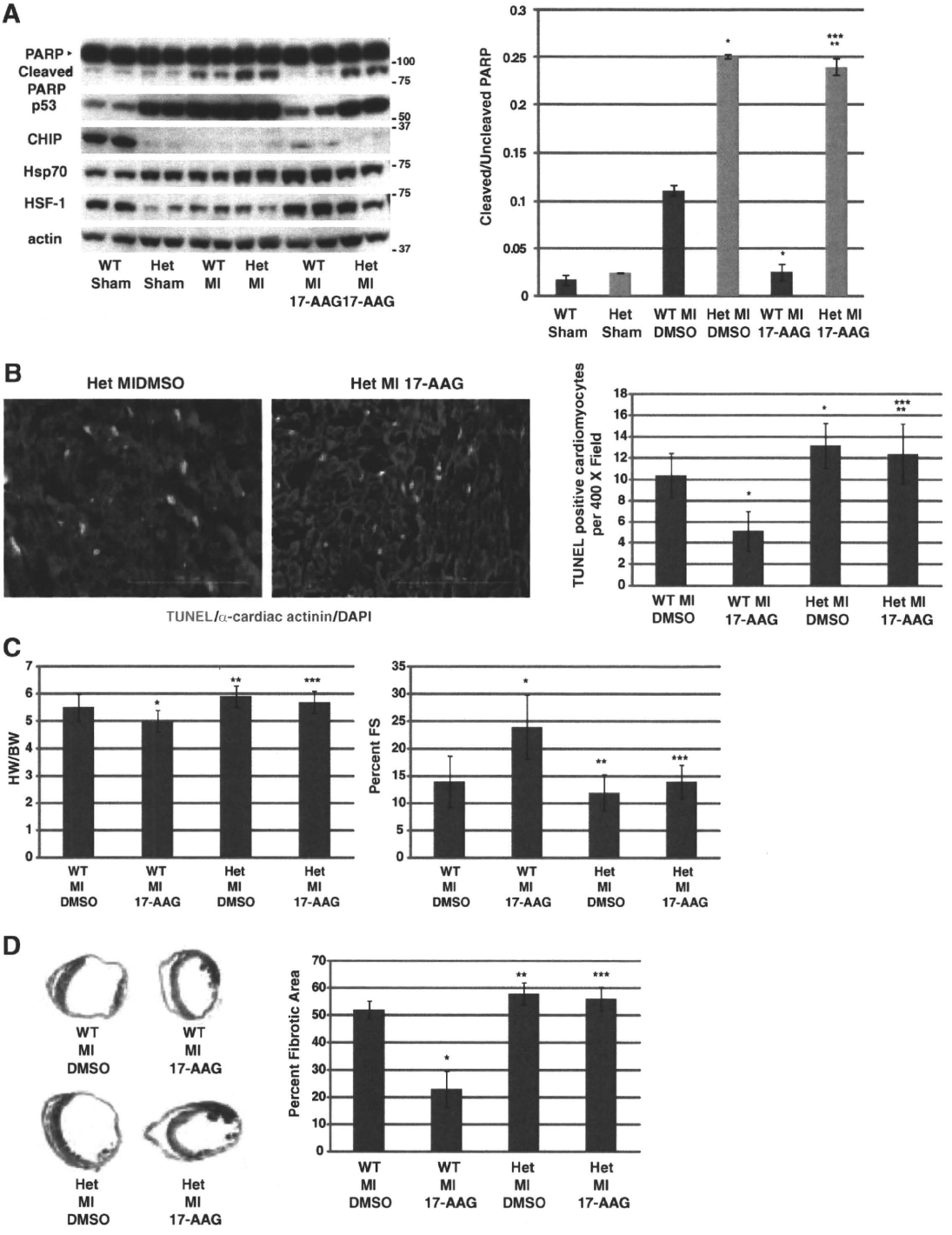

Figure 7. The effect of 17-AAG was dependent on CHIP-mediated p53 degradation and upregulation of heat shock proteins. A, 17-AAG–induced reduction of p53 accumulation and PARP expression was not observed in the heart of CHIP heterozygous mice (Het). Notably, upregulation of heat shock proteins by 17-AAG was ameliorated in CHIP heterozygous mice. **B,** Apoptotic cardiomyocytes on 1 day after MI was reduced in 17-AAG–treated mice, but this antiapoptotic effect of 17-AAG after MI was ameliorated in CHIP heterozygous mice. Apoptosis was assessed by cleaved PARP expression **(A)** and TUNEL staining **(B)**. *$P<0.01$ vs WT+MI+DMSO; **$P<0.01$ vs WT+MI +17-AAG; ***P=NS vs Het+MI+DMSO n=5. WT indicates wild-type mice; Het, CHIP heterozygous mice. **C,** 17-AAG–induced attenuation of postinfarct cardiac remodeling is less in CHIP hetero knockout mice than in wild-type mice. HW/BW ratio **(C, left)**, contractile function **(C, right)**, and fibrotic area **(D)**. *$P<0.001$; **$P<0.05$ vs WT+MI+DMSO; ***P=NS vs Het+MI+DMSO. WT+MI+DMSO: n=30; WT+MI +17-AAG: n=20; Het+MI+DMSO: n=15; Het+MI +17-AAG: n=15. WT indicates wild-type mice.

Table. Basal Characterization of the Mice Used in this Study

	Body Weight (g)	LVEDD (mm)	LVESD (mm)	IVS (mm)	LVPW (mm)	%FS
Wild type	26.3±1.2	3.12±0.12	1.04±0.02	0.72±0.02	0.74±0.02	66.7±1.3
CHIP hetero KO	25.6±0.8	3.10±0.08	1.05±0.03	0.74±0.03	0.78±0.02	66.1±0.8
CHIP Tg	26.9±1.5	3.14±0.16	1.05±0.04	0.75±0.02	0.75±0.05	66.6±1.8

suggest that hypoxic stress downregulates CHIP, leading to decreased CHIP-mediated proteolysis of p53 protein and accumulation of p53 protein. This mechanism seems to be a 'fine-tuning' of HIF-1 activity because p53 protein has been reported to bind to and inhibit HIF-1 activity.[16] After hypoxia, first HIF-1 accumulates and induces angiogenic genes, to promote angiogenesis. Thereafter, as a negative feedback loop, HIF-1 induces downregulation of *CHIP* expression and p53 accumulates, then accumulated p53 inhibits HIF-1 activity.[35] In general, this feedback system might have an antitumor effect, because in many tumor cells HIF-1 induces feeding vessels in hypoxic tumors and promotes tumor growth. HIF-1-induced, CHIP-mediated p53 accumulation acts to suppress tumor growth by (1) suppressing HIF-1 activity and blocking neovascularization and (2) inducing p53-mediated apoptosis of tumor cells. However, in the heart, this negative feedback system worsens hypoxic situation by blocking neovascularization[16] and by inducing apoptosis (this study).

The important role of apoptosis in the progression of ventricular remodeling and the possibility of antiapoptotic approach against heart failure has already been elegantly shown by Wencker et al.[3] Antiapoptotic approach after myocardial infarction has been reported to be cardioprotective not only in ischemia-reperfusion model but also in permanent coronary ligation model.[21,36,37] Therefore, inhibition of apoptotic death does not only reduce initial infarct size but also prevents ventricular remodeling through inhibiting apoptosis in the border zone of the infarct.

Accumulation of p53 has been reported to initiate many proapoptotic triggers.[38] In the heart, p53 accumulates (Figure 3C) and p53-dependent apoptosis occurs[39] after permanent coronary occlusion. We have also observed that *p53* gene deletion lead to less ventricular remodeling after myocardial infarction.[16] In the present study, we have shown that CHIP overexpression or 17-AAG treatment could prevent cardiomyocyte apoptosis and ameliorate ventricular remodeling after myocardial infarction. We have also shown some evidences that inhibition of p53 accumulation is at least one of the mechanisms for the effect of CHIP overexpression and 17-AAG. However, it should be noted that Hsp90 chaperones various proteins including prosurvival factors such as Akt/protein kinase B[40] in tumor cells and that Hsp90 inhibitors induced degradation of aberrantly overexpressed prosurvival factors in those tumor cells. Although the nature of the effects of 17-AAG seems to induce degradation of aberrantly expressed proteins, it is also possible and taken into account that 17-AAG could also induce degradation of prosurvival factors and play detrimental effects in cardiomyocytes.

In conclusion, our observations indicate that investigation of novel anti-p53 approach would open a way toward new treatment of myocardial infarction.

Acknowledgments

We thank Y. Ohtsuki, I. Sakamoto, M. Ikeda, and A. Furuyama for excellent technical support.

Sources of Funding

This work was supported by a Grant-in-Aid for Scientific Research on Priority Areas and for Exploratory Research (Ministry of Education, Culture, Sports, Science and Technology), Health and Labour Sciences Research grants (to I.K.), and research fellowships from the Japan Society for the Promotion of Science for Young Scientists (to A.T.N.). A.T.N. is a research fellow of the Japan Society for the Promotion of Science.

Disclosures

None.

References

1. Rosamond W, Flegal K, Friday G, Furie K, Go A, Greenlund K, Haase N, Ho M, Howard V, Kissela B, Kittner S, Lloyd-Jones D, McDermott M, Meigs J, Moy C, Nichol G, O'Donnell CJ, Roger V, Rumsfeld J, Sorlie P, Steinberger J, Thom T, Wasserthiel-Smoller S, Hong Y. Heart disease and stroke statistics–2007 update: a report from the American Heart Association Statistics Committee and Stroke Statistics Subcommittee. *Circulation*. 2007;115:e69–e171.
2. Kajstura J, Cheng W, Reiss K, Clark WA, Sonnenblick EH, Krajewski S, Reed JC, Olivetti G, Anversa P. Apoptotic and necrotic myocyte cell deaths are independent contributing variables of infarct size in rats. *Lab Invest*. 1996;74:86–107.
3. Wencker D, Chandra M, Nguyen K, Miao W, Garantziotis S, Factor SM, Shirani J, Armstrong RC, Kitsis RN. A mechanistic role for cardiac myocyte apoptosis in heart failure. *J Clin Invest*. 2003;111:1497–1504.
4. Haunstetter A, Izumo S. Toward antiapoptosis as a new treatment modality. *Circ Res*. 2000;86:371–376.
5. Chatterjee S, Stewart AS, Bish LT, Jayasankar V, Kim EM, Pirolli T, Burdick J, Woo YJ, Gardner TJ, Sweeney HL. Viral gene transfer of the antiapoptotic factor Bcl-2 protects against chronic postischemic heart failure. *Circulation*. 2002;106:I212–I217.
6. Hochhauser E, Kivity S, Offen D, Maulik N, Otani H, Barhum Y, Pannet H, Shneyvays V, Shainberg A, Goldshtaub V, Tobar A, Vidne BA. Bax ablation protects against myocardial ischemia-reperfusion injury in transgenic mice. *Am J Physiol Heart Circ Physiol*. 2003;284:H2351–H2359.
7. Imahashi K, Schneider MD, Steenbergen C, Murphy E. Transgenic expression of Bcl-2 modulates energy metabolism, prevents cytosolic acidification during ischemia, and reduces ischemia/reperfusion injury. *Circ Res*. 2004;95:734–741.
8. Hochhauser E, Cheporko Y, Yasovich N, Pinchas L, Offen D, Barhum Y, Pannet H, Tobar A, Vidne BA, Birk E. Bax deficiency reduces infarct size and improves long-term function after myocardial infarction. *Cell Biochem Biophys*. 2007;47:11–20.
9. Vogelstein B, Lane D, Levine AJ. Surfing the p53 network. *Nature*. 2000;408:307–310.
10. Haupt Y, Maya R, Kazaz A, Oren M. Mdm2 promotes the rapid degradation of p53. *Nature*. 1997;387:296–299.
11. Kubbutat MH, Jones SN, Vousden KH. Regulation of p53 stability by Mdm2. *Nature*. 1997;387:299–303.
12. Dornan D, Wertz I, Shimizu H, Arnott D, Frantz GD, Dowd P, O'Rourke K, Koeppen H, Dixit VM. The ubiquitin ligase COP1 is a critical negative regulator of p53. *Nature*. 2004;429:86–92.
13. Leng RP, Lin Y, Ma W, Wu H, Lemmers B, Chung S, Parant JM, Lozano G, Hakem R, Benchimol S. Pirh2, a p53-induced ubiquitin-protein ligase, promotes p53 degradation. *Cell*. 2003;112:779–791.
14. Long X, Boluyt MO, Hipolito ML, Lundberg MS, Zheng JS, O'Neill L, Cirielli C, Lakatta EG, Crow MT. p53 and the hypoxia-induced apoptosis

of cultured neonatal rat cardiac myocytes. *J Clin Invest.* 1997;99:2635–2643.
15. Liu P, Xu B, Cavalieri TA, Hock CE. Pifithrin-alpha attenuates p53-mediated apoptosis and improves cardiac function in response to myocardial ischemia/reperfusion in aged rats. *Shock.* 2006;26:608–614.
16. Sano M, Minamino T, Toko H, Miyauchi H, Orimo M, Qin Y, Akazawa H, Tateno K, Kayama Y, Harada M, Shimizu I, Asahara T, Hamada H, Tomita S, Molkentin JD, Zou Y, Komuro I. p53-induced inhibition of Hif-1 causes cardiac dysfunction during pressure overload. *Nature.* 2007;446:444–448.
17. Song K, Backs J, McAnally J, Qi X, Gerard RD, Richardson JA, Hill JA, Bassel-Duby R, Olson EN. The transcriptional coactivator CAMTA2 stimulates cardiac growth by opposing class II histone deacetylases. *Cell.* 2006;125:453–466.
18. Zou Y, Komuro I, Yamazaki T, Kudoh S, Uozumi H, Kadowaki T, Yazaki Y. Both Gs and Gi proteins are critically involved in isoproterenol-induced cardiomyocyte hypertrophy. *J Biol Chem.* 1999;274:9760–9770.
19. Sohal DS, Nghiem M, Crackower MA, Witt SA, Kimball TR, Tymitz KM, Penninger JM, Molkentin JD. Temporally regulated and tissue-specific gene manipulations in the adult and embryonic heart using a tamoxifen-inducible Cre protein. *Circ Res.* 2001;89:20–25.
20. Sahara N, Murayama M, Mizoroki T, Urushitani M, Imai Y, Takahashi R, Murata S, Tanaka K, Takashima A. In vivo evidence of CHIP up-regulation attenuating tau aggregation. *J Neurochem.* 2005;94:1254–1263.
21. Harada M, Qin Y, Takano H, Minamino T, Zou Y, Toko H, Ohtsuka M, Matsuura K, Sano M, Nishi J, Iwanaga K, Akazawa H, Kunieda T, Zhu W, Hasegawa H, Kunisada K, Nagai T, Nakaya H, Yamauchi-Takihara K, Komuro I. G-CSF prevents cardiac remodeling after myocardial infarction by activating the Jak-Stat pathway in cardiomyocytes. *Nat Med.* 2005;11:305–311.
22. McDonough H, Patterson C. CHIP: a link between the chaperone and proteasome systems. *Cell Stress Chaperones.* 2003;8:303–308.
23. Esser C, Scheffner M, Hohfeld J. The chaperone-associated ubiquitin ligase CHIP is able to target p53 for proteasomal degradation. *J Biol Chem.* 2005;280:27443–27448.
24. Tripathi V, Ali A, Bhat R, Pati U. CHIP chaperones wild type p53 tumor suppressor protein. *J Biol Chem.* 2007;282:28441–28454.
25. Graeber TG, Peterson JF, Tsai M, Monica K, Fornace AJ Jr, Giaccia AJ. Hypoxia induces accumulation of p53 protein, but activation of a G1-phase checkpoint by low-oxygen conditions is independent of p53 status. *Mol Cell Biol.* 1994;14:6264–6277.
26. An WG, Kanekal M, Simon MC, Maltepe E, Blagosklonny MV, Neckers LM. Stabilization of wild-type p53 by hypoxia-inducible factor 1alpha. *Nature.* 1998;392:405–408.
27. Chen KF, Lai YY, Sun HS, Tsai SJ. Transcriptional repression of human cad gene by hypoxia inducible factor-1alpha. *Nucleic Acids Res.* 2005;33:5190–5198.
28. Eltzschig HK, Abdulla P, Hoffman E, Hamilton KE, Daniels D, Schonfeld C, Loffler M, Reyes G, Duszenko M, Karhausen J, Robinson A, Westerman KA, Coe IR, Colgan SP. HIF-1-dependent repression of equilibrative nucleoside transporter (ENT) in hypoxia. *J Exp Med.* 2005;202:1493–1505.
29. Ibla JC, Khoury J, Kong T, Robinson A, Colgan SP. Transcriptional repression of Na-K-2Cl cotransporter NKCC1 by hypoxia-inducible factor-1. *Am J Physiol Cell Physiol.* 2006;291:C282–C289.
30. Bindra RS, Glazer PM. Co-repression of mismatch repair gene expression by hypoxia in cancer cells: role of the Myc/Max network. *Cancer Lett.* 2007;252:93–103.
31. Waza M, Adachi H, Katsuno M, Minamiyama M, Sang C, Tanaka F, Inukai A, Doyu M, Sobue G. 17-AAG, an Hsp90 inhibitor, ameliorates polyglutamine-mediated motor neuron degeneration. *Nat Med.* 2005;11:1088–1095.
32. Dickey CA, Kamal A, Lundgren K, Klosak N, Bailey RM, Dunmore J, Ash P, Shoraka S, Zlatkovic J, Eckman CB, Patterson C, Dickson DW, Nahman NS Jr, Hutton M, Burrows F, Petrucelli L. The high-affinity HSP90-CHIP complex recognizes and selectively degrades phosphorylated tau client proteins. *J Clin Invest.* 2007;117:648–658.
33. Suzuki K, Sawa Y, Kaneda Y, Ichikawa H, Shirakura R, Matsuda H. In vivo gene transfection with heat shock protein 70 enhances myocardial tolerance to ischemia-reperfusion injury in rat. *J Clin Invest.* 1997;99:1645–1650.
34. Sakamoto M, Minamino T, Toko H, Kayama Y, Zou Y, Sano M, Takaki E, Aoyagi T, Tojo K, Tajima N, Nakai A, Aburatani H, Komuro I. Upregulation of heat shock transcription factor 1 plays a critical role in adaptive cardiac hypertrophy. *Circ Res.* 2006;99:1411–1418.
35. Blagosklonny MV, An WG, Romanova LY, Trepel J, Fojo T, Neckers L. p53 inhibits hypoxia-inducible factor-stimulated transcription. *J Biol Chem.* 1998;273:11995–11998.
36. Chandrashekhar Y, Sen S, Anway R, Shuros A, Anand I. Long-term caspase inhibition ameliorates apoptosis, reduces myocardial troponin-I cleavage, protects left ventricular function, and attenuates remodeling in rats with myocardial infarction. *J Am Coll Cardiol.* 2004;43:295–301.
37. Balsam LB, Kofidis T, Robbins RC. Caspase-3 inhibition preserves myocardial geometry and long-term function after infarction. *J Surg Res.* 2005;124:194–200.
38. Crow MT, Mani K, Nam YJ, Kitsis RN. The mitochondrial death pathway and cardiac myocyte apoptosis. *Circ Res.* 2004;95:957–970.
39. Matsusaka H, Ide T, Matsushima S, Ikeuchi M, Kubota T, Sunagawa K, Kinugawa S, Tsutsui H. Targeted deletion of p53 prevents cardiac rupture after myocardial infarction in mice. *Cardiovasc Res.* 2006;70:457–465.
40. Solit DB, Basso AD, Olshen AB, Scher HI, Rosen N. Inhibition of heat shock protein 90 function downregulates Akt kinase and sensitizes tumors to Taxol. *Cancer Res.* 2003;63:2139–2144.

Novelty and Significance

What Is Known?

- Inhibition of myocardial apoptosis after myocardial infarction is cardioprotective.
- p53 expression is increased after myocardial infarction and induces cardiomyocyte apoptosis.

What New Information Does This Article Contribute?

- We identified CHIP as the endogenous p53 antagonist expressed in the heart.
- We found that CHIP downregulation is critically involved in the molecular mechanisms for p53 elevation after myocardial infarction.
- We showed several possibilities of the anti-p53 treatment after myocardial infarction.

Accumulation of tumor suppressor protein p53 in the myocardium causes the transition from adaptive cardiac hypertrophy to heart failure. However, the mechanisms of p53 accumulation in the heart and its therapeutic implications have been elusive. Here we show that downregulation of the chaperone-associated E3 ubiquitin ligase CHIP (carboxyl terminus of Hsp70-interacting protein) mediates hypoxia-induced p53 accumulation in the heart and that promotion of CHIP-induced p53 degradation protects the heart from ischemic injury. Under physiological conditions, CHIP limited the p53 protein amount at low levels by inducing proteasomal degradation of p53. Under hypoxic conditions, hypoxia inducible factor-1 (HIF-1) down-regulated CHIP, resulting in the accumulation of p53. Overexpression of CHIP or administration of an Hsp90 inhibitor promoted CHIP-mediated p53 degradation and attenuated ischemic cardiac injury. These results indicate that CHIP is a crucial negative regulator of p53 in the heart and suggest that promotion of CHIP-mediated p53 degradation could be a novel therapeutic strategy for heart diseases.

Original Article

Fenofibrate Reduces Postprandial Hypertriglyceridemia in CD36 Knockout Mice

José C. Sandoval[1], Yumiko Nakagawa-Toyama[2], Daisaku Masuda[1], Yoshihiro Tochino[3], Hajime Nakaoka[1], Ryota Kawase[1], Miyako Yuasa-Kawase[1], Kazuhiro Nakatani[1], Miwako Inagaki[1], Kazumi Tsubakio-Yamamoto[1], Tohru Ohama[1], Makoto Nishida[2], Masato Ishigami[4], Issei Komuro[1], and Shizuya Yamashita[1]

[1]Department of Cardiovascular Medicine, Osaka University Graduate School of Medicine, Osaka, Japan
[2]Health Care Center, Osaka University, Osaka, Japan
[3]Department of Metabolic Medicine, Osaka University Graduate School of Medicine, Osaka, Japan
[4]Department of Biomedical Informatics, Division of Health Sciences, Osaka University Graduate School of Medicine, Osaka, Japan

Aim: Metabolic syndrome (MetS) and postprandial hypertriglyceridemia (PHTG) are closely related and both are associated with coronary heart disease. We have demonstrated that CD36 deficiency is prevalent in the genetic background of MetS and is accompanied by PHTG concomitantly with an increase in remnants and a decrease in high density lipoprotein cholesterol. These findings make CD36 knockout mice (CD36KO) an interesting model for evaluating PHTG in MetS. Fenofibrate was reported to reduce fasting and postprandial triglyceride (TG) levels in hypertriglyceridemic subjects with MetS. To define its mechanism, we investigated the effect of fenofibrate on PHTG in CD36KO.

Methods: Wild-type (WT) and CD36KO mice were fed chow diet and fenofibrate for two weeks. TG concentrations and lipoprotein profiles were assessed during fasting and in the postprandial state in plasma; intestinal mucosa and lymph were collected after oral fat loading for both treatment groups.

Results: Fenofibrate treatment markedly suppressed the postprandial TG response in CD36KO along with decreased apoB-48 levels in plasma. HPLC analysis depicted the decrease of TG content in chylomicrons (CM) and CM remnant-sized lipoproteins contributed to this suppression, suggesting that CM and CM remnant production in the intestines might be attenuated by fenofibrate. ApoB-48 and TG levels in intestinal lymph were markedly reduced after treatment. Intestinal mRNA expression of apoB was also reduced in the postprandial state after fenofibrate administration without affecting any other genes related to CM assembly and production.

Conclusion: Fenofibrate reduces PHTG in CD36KO partially through attenuating intestinal CM production.

J Atheroscler Thromb, 2010; 17:610-618.

Key words; Fenofibrate, Postprandial hypertriglyceridemia, CD36 knockout mice, Apolipoprotein B-48

Introduction

Metabolic syndrome (MetS), based upon the accumulation of visceral fat, represents a clustering of interrelated risk factors for cardiovascular disease that include abnormally high serum triglyceride (TG) levels in the fasting state[1, 2]. Metabolic syndrome presents as a challenge to the healthcare system, particularly due to the increasing prevalence of overweight/obesity and type 2 diabetes mellitus worldwide[3].

The publication of meta-analyses pointing at raised serum TG levels as an independent risk factor for coronary heart disease highly suggests that TG-rich lipoproteins, such as chylomicrons (CM), very low

Address for correspondence: Shizuya Yamashita, Department of Cardiovascular Medicine, Osaka University Graduate School of Medicine, 2-2 Yamada-oka, Suita, Osaka 565-0871, Japan
E-mail: shizu@imed2.med.osaka-u.ac.jp
Received: October 20, 2009
Accepted for publication: November 24, 2009

density lipoproteins (VLDL) and their remnants, are atherogenic[4, 5]. Triglycerides are routinely measured in the fasting state, excluding CM and their remnants; however, elevated non-fasting TG levels were found to be associated with an increased risk of coronary artery disease, stroke and death in men and women[6-8], which suggests atherosclerosis as a postprandial phenomenon where CM and CM remnants would play an important role. Thus, increased levels of non-fasting TG, as well as increased levels of CM and CM remnants, should constitute a potentially important predictor of atherosclerotic cardiovascular diseases, and the strong evidence supporting the independent atherogenicity of these remnants[9] makes them appropriate targets for lipid-lowering therapy.

CD36, also known as fatty acid (FA) translocase, an 88 kD glycoprotein belonging to the scavenger receptor class B, has been shown to bind multiple ligands, including long-chain FAs and oxidized low density lipoproteins[10]. CD36 is broadly expressed in many cells, such as monocytes, platelets, macrophages, microvascular endothelial cells, adipocytes, skeletal and cardiac myocytes, enterocytes and Kupffer cells[11]. Human CD36 deficiency is accompanied by multiple risk factors, such as increased remnant lipoproteins and low high density lipoproteins (HDL) cholesterol, as well as impaired glucose metabolism, based upon insulin resistance. These findings suggested that this condition may be considered a genetic background for MetS[12, 13]. CD36 knockout (CD36KO) mice have been also demonstrated to increase the postprandial plasma TG and FA response after an acute oral fat loading of more than 2-fold compared to wild-type (WT) mice[14]. We demonstrated a postprandial increase of plasma CM-remnants with enhanced TG synthesis in the small intestine of CD36KO compared to WT mice and suggested that the main cause for the postprandial elevation of TG in plasma was the *de novo* synthesis of small-sized CM in enterocytes[15]. These findings strongly suggest CD36KO mice as an interesting model to evaluate postprandial hypertriglyceridemia in a MetS environment.

Peroxisome proliferator activated receptor (PPAR) alpha is a ligand-activated transcription factor with diverse functions, expressed in a variety of tissues[16], and is activated by several synthetic compounds. Fenofibrate, a PPAR-α ligand, has been demonstrated to reduce TG levels in fasting and postprandial states in a cohort of hypertriglyceridemic subjects with MetS; this TG-lowering effect resulted primarily from reductions in fasting and postprandial concentrations of large and medium VLDL particles[17]. Moreover, fenofibrate has been shown to reduce non-fatal myocardial infarctions and coronary revascularizations in diabetic patients[18].

To elucidate the effect of fenofibrate on postprandial hypertriglyceridemia in CD36KO mice, we performed an oral fat-loading test before and after fenofibrate treatment and demonstrated that fenofibrate reduced postprandial hypertriglyceridemia, thus promoting a protective effect against atherosclerosis in a mouse model for MetS.

Materials and Methods

Animals

Male CD36KO mice created on a C57BL6/J background, which were kindly provided by Mason. W. Freeman, M.D., Ph.D., Professor of Harvard Medical School[19], and C57BL6/J WT mice at 8-10 weeks of age were used for this experiment. Each strain of mice was separated into two groups, which were fed chow diet (MF, Oriental BioLaboratories, Chiba, Japan) alone or chow diet containing 0.05% fenofibrate (Aska Pharmaceuticals, Tokyo, Japan) for 2 weeks. The mice were housed in a temperature-controlled environment with a 12-hour dark-light cycle and free access to food and water. The experimental protocol was approved by the Ethics Review Committee for Animal Experimentation of Osaka University Graduate School of Medicine (IEXAS). After 2 weeks of treatment, each strain was fasted for 12 hours and separated into two groups to be euthanized: in the fasting state and three hours after acute ingestion of 17 μL/g body weight of olive oil (Nacalai Tesque, Kyoto, Japan) by gavaging.

Triglyceride Determination and Lipoprotein Analysis of Plasma and Intestinal Lymph

Plasma and lymph TG concentrations were measured enzymatically (Wako Pure Chemical Industries, Tokyo, Japan) according to the manufacturer's protocol.

The plasma and lymph lipoprotein profile was analyzed by an online dual enzymatic method using high performance liquid chromatography (HPLC) at Skylight Biotech Inc. (Akita, Japan)[20], where 200 μL of plasma or lymph were dissolved in loading buffer and loaded onto TSK gel Lipopropak XL columns. Triglyceride concentrations in the flow-through were measured continuously and simultaneously. The correspondence of lipoprotein fractions (CM, VLDL, LDL, and HDL-sized fractions) and the elution time were CM (>80 nm, fraction time: 15-17 min), VLDL (30-80 nm, fraction time: 17-22 min), LDL (16-30 nm, fraction time: 22-28 min), and HDL (8-16 nm,

fraction time: 28–37 min).

Collection of Intestinal Lymph in the Postprandial State

Five mice from each strain were loaded with olive oil (17 μL/g body weight) after a fasting period of 12 hours. Three hours later, mice were anesthetized and the intestinal lymphatic trunk was cannulated using a 27-gauge needle inserted into a polyethylene tube (PE-50) previously flushed with EDTA-treated water, according to the modified method described by Bollman *et al.*[21].

Western Blot

One microliter of plasma or lymph was subjected to 4–12% SDS-polyacrylamide gel electrophoresis (SDS-PAGE; TEFCO, Tokyo, Japan), transferred onto an Immobilon-P transfer membrane (Millipore Corp., USA) and blocked by Blocking One (Nacalai Tesque, Kyoto, Japan). The membrane was then incubated with anti-mouse apoB-48/B-100 antibody (BIODESIGN International, ME, USA) and anti-rabbit IgG antibody (NA934V; GE Healthcare Backinghamshire, UK). Bands corresponding to apoB-100 and apoB-48 were detected with the ECL Advance Detection Kit (GE Healthcare, UK).

RNA Extraction, cDNA Synthesis and Quantitative Real-Time PCR

The small intestine from each animal was removed, flushed with ice-cold phosphate-buffered saline and divided into three sections of equal length, the proximal two-thirds of the mucosa was gently scraped and stored in RNAlater RNA stabilization reagent (QIAGEN GmbH, Germany) at −20℃.

Total RNA from tissue samples was extracted and purified using the RNeasy Lipid Tissue Mini Kit (cat. 70804; QIAGEN GmbH, Germany). One microgram of the total RNA was primed with 50 pmol of oligo (dT) 20 and transcripted with Superscript Ⅲ (Invitrogen, CA, USA) for first-strand cDNA synthesis, according to the manufacturer's protocol. qRT-PCR was performed; DNA polymerase and SYBR Green I (Finnzymes Oy, Espoo, Finland) were set in a reaction volume of 20 μL containing gene-specific primers (5 μM) and cDNA (corresponding to ~50 ng total RNA). The reaction was performed using the DNA engine Opticon 2 real-time PCR detection system (Bio-Rad Laboratories, Hercules, CA). The $2^{-\Delta\Delta CT}$ method of relative gene expression was employed and a standard deviation of ct value of <0.3 was accepted. Results are expressed as arbitrary units in comparison with the expression of GAPDH.

Primers for this Study

The sequence data of the genes were found in GenBank and the sequences of primers were designed with Primer3 (http://frodo.wi.mit.edu/cgi-bin/primer3/primer3_www.cgi). GAPDH was used as a housekeeping gene. The sequence and information for primers used in this study are as follows: FATP-4 (GenBank accession number NM_011989): 5'-atcaacaccaaccttaggcg-3' and 5'-aacccttgtctgggtgactg-3', FABP1 (NM_017399): 5'-catccagaaagggaaggaca-3' and 5'-ttttcccc-agtcatggtctc-3', FABP2 (NM_007980): 5'-ttgctgtccgag-aggtttct-3' and 5'-gctttgacaaggctggagac-3', DGAT-1 (NM_010046): 5'-gtgcacaagtggtgcatcag-3' and 5'-cag-tgggatctgagccatc-3', DGAT-2 (NM_026384): 5'-agtg-gcaatgctatcatcatcgt-3' and 5'-aaggaataagtgggaacca-gatca-3', MGAT-2 (NM_177448): 5'-gaagaagcagcat-cagggac-3' and 5'-gtgtgggattaggggactt-3', ApoB (NM_009693): 5'-tgggattccatctgccatctcgag-3' and 5'-gtaga-gatccatcacaggacaatg-3', MTTP (NM_008642): 5'-cat-gtcagccatcctgtttg-3' and 5'-ctcgcgataccacagactga-3', and GAPDH (NM_008084): 5'-actccactcacggcaaa-ttc-3' and 5'-tctccatggtggtgaagaca-3'.

Statistical Analysis

The values are expressed as the means ± S.D. Statistical significance was assessed by Student's *t*-test for paired values and set at $p<0.05$.

Results

Fenofibrate Reduces Postprandial Hypertriglyceridemia, as well as ApoB-100 and ApoB-48 Mass in Wild-Type and CD36KO Mice in Fasting and Postprandial States

CD36KO mice showed significantly higher plasma TG levels than WT controls (638 ± 123 mg/dL vs. 168 ± 27 mg/dL, $p<0.05$) in the postprandial state (**Fig. 1**). Administration of fenofibrate decreased plasma TG concentrations in the fasting state in both WT (87 ± 32 vs. 21 ± 2 mg/dL, $p<0.05$) and CD36KO mice (82 ± 11 vs. 23 ± 4 mg/dL, $p<0.05$). Moreover, fenofibrate markedly reduced the postprandial plasma TG concentration in CD36KO mice (638 ± 123 vs. 45 ± 20 mg/dL, $p<0.05$), while the reduction of TG in WT mice was somewhat modest compared to that in CD36KO mice (168 ± 27 vs. 52 ± 14 mg/dL, $p<0.05$). This marked diminution of the TG level in the postprandial state in CD36KO mice after fenofibrate treatment implies that fenofibrate could act more efficiently in the postprandial state in the MetS environment. It is important to point out that fenofibrate administration did not affect mouse weight significantly during the 2-week treatment in both CD36KO

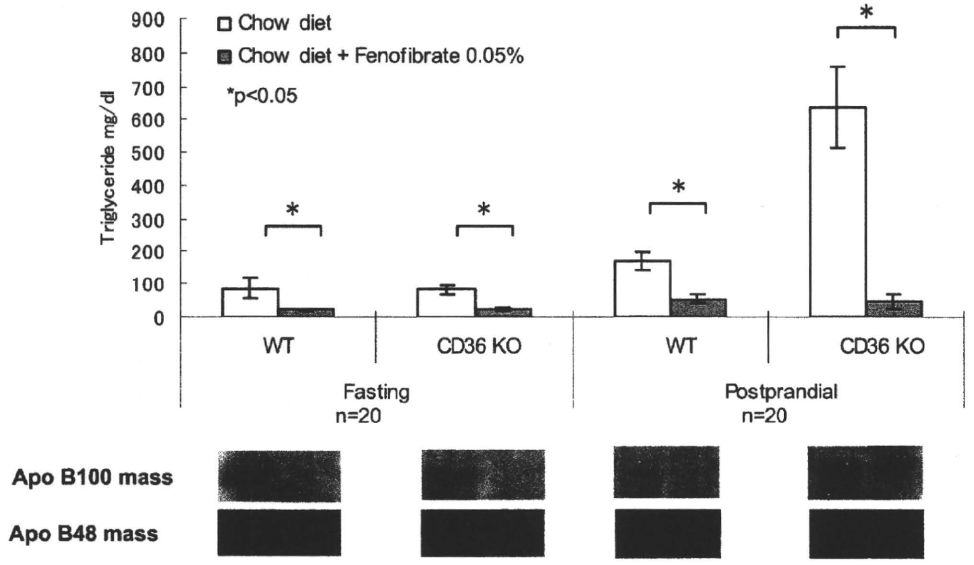

Fig. 1. Fenofibrate decreased plasma TG levels in CD36 knockout and WT mice in fasting and postprandial states.

(Upper panel) Addition of fenofibrate (gray) showed a significant decrease in TG levels in fasting and postprandial states in WT and CD36KO mice; the TG reductions for WT and CD36KO mice were 3.2 and 13.9 times, respectively. ($p < 0.05$)

(Lower panel) Representative Western blot images of apoB-100 and apoB-48 masses loaded the same amount of plasma in each subgroup.

and WT groups compared to their chow diet controls (data not shown).

To assess the effect of fenofibrate administration on apoB-48 mass in the plasma of WT and CD36KO mice in fasting and postprandial states, Western blotting was performed. The amount of both apolipoprotein B isoforms, apoB-100 and apoB-48, in plasma was markedly reduced after fenofibrate treatment in both states and strains (**Fig. 1**), implying that both apoB-100- and apoB-48-containing lipoproteins were reduced.

Fenofibrate Reduces Postprandial CM and VLDL-Sized Particles in Plasma of CD36KO Mice

The plasma lipoprotein profile was analyzed by automatic HPLC using a pool of 3 samples for each group. CD36KO mice showed a marked increase in postprandial TG levels of every lipoprotein fraction compared to their WT controls before fenofibrate administration. Among subfractions, a substantial difference between CD36KO and WT mice was demonstrated in TG levels of CM and VLDL-sized particles, which also include CM remnants, indicating that CD36KO mice showed impaired TG-rich lipoprotein metabolism in the postprandial state (**Fig. 2A**). Fenofibrate reduced postprandial TG levels in WT and CD36KO mice mainly in these subfractions (**Fig. 2B, 2C**). **Fig. 2D** shows the overall HPLC analysis of CD36KO mouse plasma in the postprandial state before and after fenofibrate treatment. These results raised the possibility that fenofibrate could modulate intestinal CM production. Thus, we further investigated the lipoproteins in the intestinal lymph and intestinal mRNA expression of genes in CD36KO mice in the postprandial state before and after fenofibrate treatment.

Fenofibrate Reduces Postprandial TG and ApoB-48 Mass in Intestinal Lymph of CD36KO Mice

Fenofibrate significantly reduced the postprandial TG concentration in the intestinal lymph of CD36KO mice in the postprandial state (18.6 ± 2.2 vs. 10.0 ± 1.6 g/dL, $p < 0.05$) accompanied by a decrease in ApoB-48 mass (**Fig. 3A**). The highest peak in TG levels corresponded to the CM fraction in both treated and non-treated mice, with a discrete elevation in the VLDL-sized fraction, which corresponds to CM remnants, since the obtained lymph lacked apoB-100 (**Fig. 3B**). Fenofibrate decreased both CM and CM remnant-sized curves, suggesting that fenofibrate might decrease the production of intestine-derived lipoproteins in the postprandial state in CD36KO mice (**Fig. 3B**).

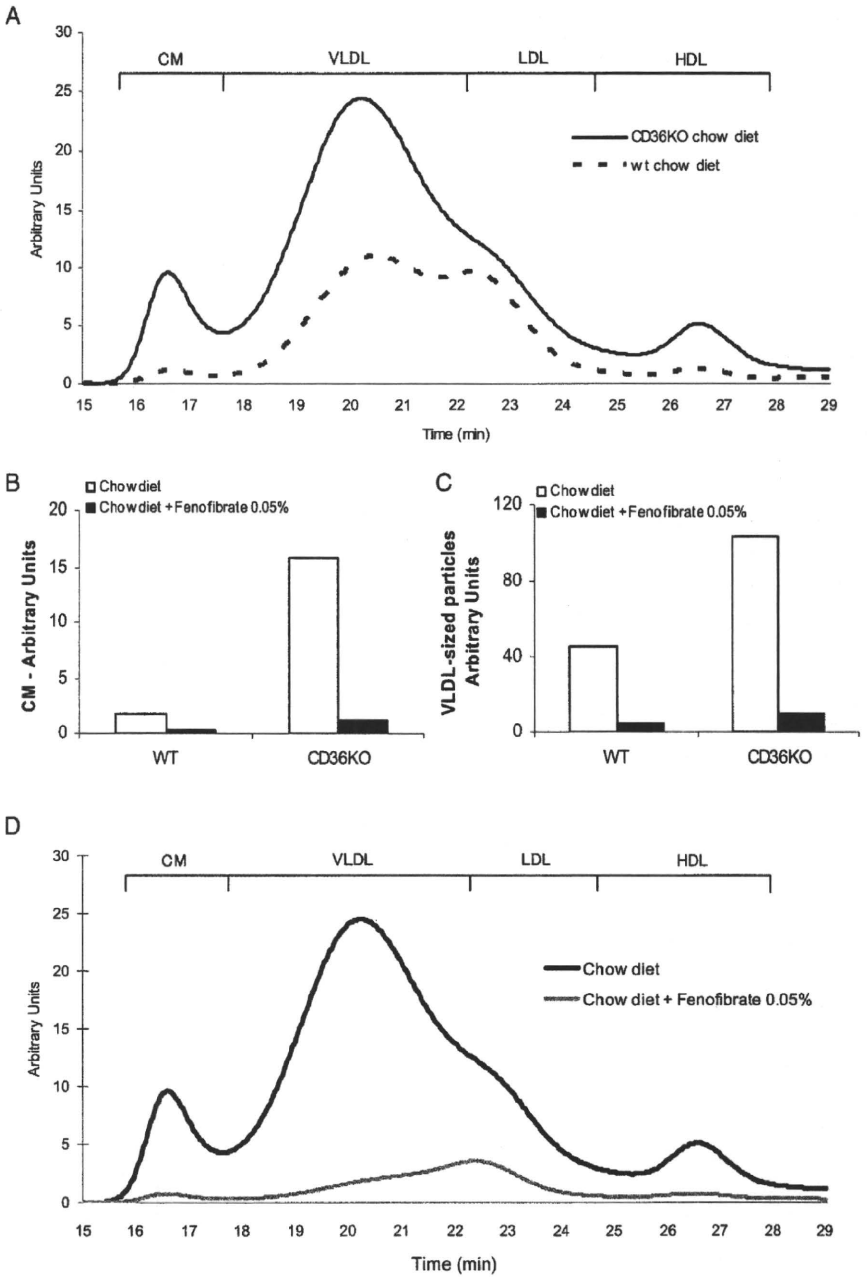

Fig. 2. Effects of fenofibrate on lipoprotein fractions in plasma of CD36KO mice in postprandial state.

(A) HPLC performed on plasma showed a higher 3-hour postprandial TG response of CD36KO (solid line) than WT mice (dashed line). Fenofibrate treatment (black) decreased postprandial plasma TG levels in CM (B) and VLDL-sized particles which also include CM remnants (C). (D) Plasma HPLC curves in postprandial state before (solid black line) and after (solid gray line) fenofibrate treatment in CD36KO mice

Fenofibrate is Involved in the Transcriptional Regulation of Lipid Metabolism-Related Genes in Intestine of CD36KO Mice in Postprandial State

To determine the possible mechanisms involved in the attenuation of postprandial hypertriglyceridemia by fenofibrate, qRT-PCR using isolated total intestinal mRNA was performed and the expression of genes associated with FA and TG transport as well as

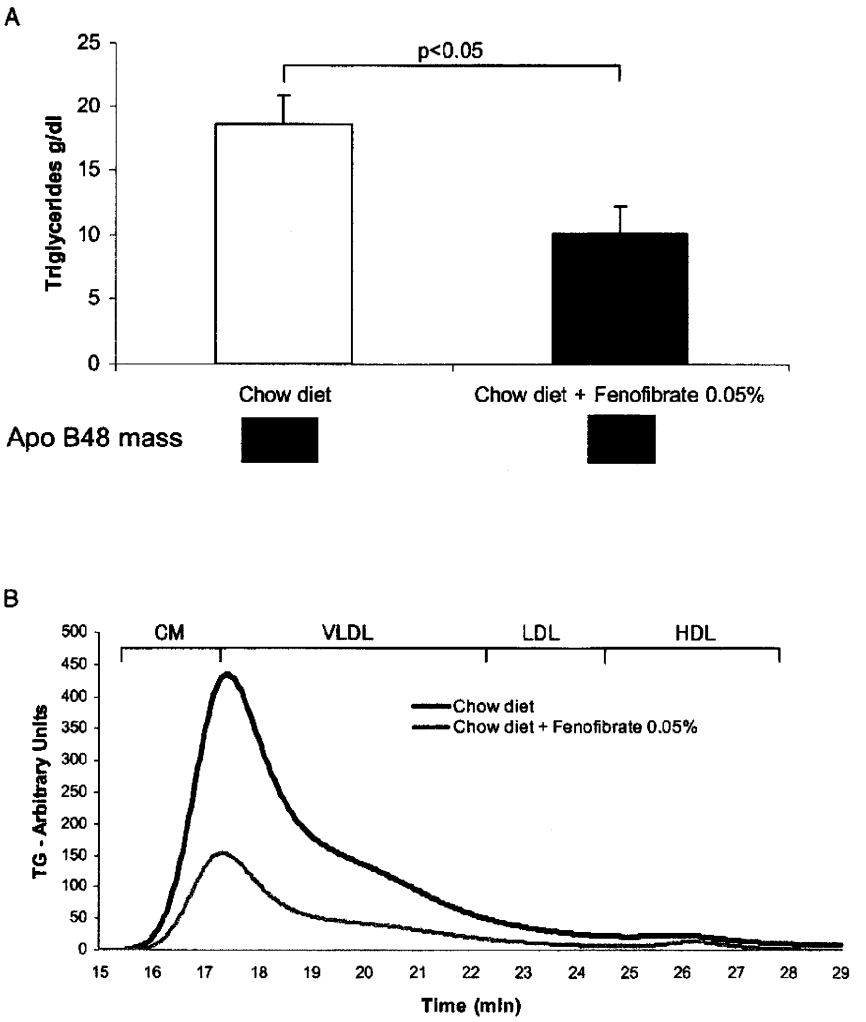

Fig. 3. Fenofibrate reduces postprandial TG and apoB-48 mass in intestinal lymph of CD36KO mice.

(A) Fenofibrate treatment (black bar) significantly reduced postprandial TG in intestinal lymph of CD36KO mice, and also notably decreased the apoB-48 mass 3 hours after the ingestion of a fat load. (B) HPLC curves of lymphatic lipoproteins in postprandial state before (solid black line) and after (solid gray line) fenofibrate treatment in CD36KO mice.

CM assembly in the intestine of CD36KO mice treated and non-treated with fenofibrate was examined. First we investigated the intestinal PPARalfa expression to confirm the efficacy of fenofibrate treatment in this experiment. Fenofibrate administrated for two weeks to CD36KO mice increased the intestinal mRNA expression of PPARalfa 2-fold.

The mRNA levels of fatty acid transport protein (FATP)-4, and fatty acid binding proteins (FABP)-1 and FABP-2, which are highly associated with the uptake and transport of long chain FAs, did not change significantly in the presence of fenofibrate. The mRNA expression of diacyl glycerol acyl transferase (DGAT)-1, DGAT-2, and monoacyl glicerol acyl transferase (MGAT)-2, which are involved in the intracellular formation of TG in intestinal epithelial cells, did not change significantly (**Fig. 4**).

ApoB mRNA was found to be decreased in mice fed with fenofibrate, while the genes that participate in apoB mRNA production, apobec-1 and apobec-1 complementation factor (ACF), were not affected significantly, which suggests the decrease of intestinal apoB mRNA as a determinant factor in the inhibitory action of fenofibrate on CM production (**Fig. 4**).

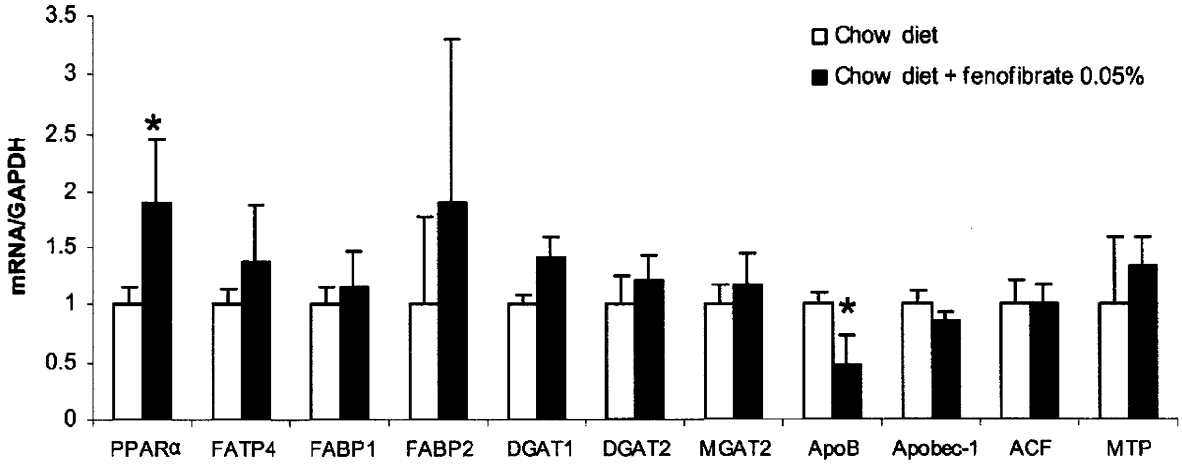

Fig. 4. Fenofibrate was involved in the transcriptional regulation of lipid metabolism-related genes in the intestine of CD36KO mice in postprandial state.

The mRNA expression of genes involved in intestinal TG manipulation and CM production were evaluated by qRT-PCR. Fenofibrate decreased apoB mRNA in CD36KO mice in postprandial state significantly ($p<0.05$). No significant difference was observed in the expression of genes that regulate apoB mRNA production, as well as in those associated with fatty acid transport, TG formation, and CM assembly.

Interestingly, microsome triglyceride transfer protein (MTP) mRNA expression, considered to have an important role in CM assembly in epithelial cells, was not significantly altered by the presence of fenofibrate.

Discussion

The TG-lowering effect of fenofibrate has been widely reported to occur mainly via the activation of lipoprotein lipase (LPL) by increased hepatic LPL mRNA levels and by suppression of liver mRNA levels of apoCIII, which is a potent inhibitor of LPL. The former was supported by the finding of a peroxisome proliferator-response element (PPRE) in the human LPL gene[22]. Fenofibrate also down-regulates lipogenic genes in the liver, such as fatty acid synthase, acetyl CoA carboxylase, and DGAT-2, inducing hepatic FA uptake and reducing FA synthesis and VLDL production in hepatocytes, thereby directly affecting the catabolism of TG-rich lipoprotein[23,24].

As described above, the mechanism of action of fenofibrate in the TG-lowering effect was largely centered on the liver and could explain in part the marked reduction of VLDL-sized CM remnants observed in the plasma of treated CD36KO mice (**Fig. 2D**). However, little is known about the effect of fenofibrate on TG metabolism in the intestine. We did not determine LPL activity in our study, already mentioned as a crucial factor in the TG-lowering effect of fenofibrate, since we focused on the mechanisms concerning the intestinal production of ApoB-containing lipoproteins. This study added a novel mechanism of the TG-lowering effect of fibrates, that is, the production of intestine-derived lipoproteins, CM and CM remnant-sized particles, was inhibited by fenofibrate (**Fig. 3B**).

It is known that CD36KO mice present an increased hypertriglyceridemic response to both oral fat loading and chronic exposure to a high fat diet compared to WT mice[14]. Our laboratory previously found an increased TG concentration and apoB-48 mass in the intestinal lymph of CD36KO mice in fasting and postprandial states, without any alteration in lipoprotein lipase (LPL) or hepatic lipase activity between CD36KO and WT mice, highly suggesting that the postprandial hypertriglyceridemia observed in this animal model is due to increased CM production from the intestine[15]. In the present study, we demonstrated that the PPAR-α agonist fenofibrate was able to decrease postprandial TG levels in plasma and intestinal lymph of CD36KO mice.

Our results also showed a statistically significant reduction in the postprandial apoB mRNA expression of CD36KO mice treated with fenofibrate, which might suggest this as the mechanism responsible for reduced CM production. However, the regulation of apoB has been largely reported to be posttranscriptional, although it is also true that most of these studies were not performed in intestinal cells but in hepa-

tocytes[25]. Fu *et al.*[26] reported the PPAR-α agonist ciprofibrate as an inhibitor of the expression of ACF, one of the responsible factors of apoB mRNA production; however, this inhibition was found only in the liver, not in the intestine of LDL-receptor knockout mice. This supports the idea that the factors involved in the regulation of apoB lipoproteins, including PPAR-α agonists, might differ between these two tissues, which leads to the need for more studies to understand the regulation of apoB in the small intestine.

MTP catalyzes the transfer of TG and cholesteryl esters to apoB and therefore has a main role in the assembly of apoB-containing lipoproteins. It has been reported that PPAR-α agonists increase MTP expression and apoB secretion in rodent liver but not in the intestine in spite of decreased plasma TG levels[27]. We found that MTP expression was not affected by fenofibrate in the intestine of CD36KO mice in the postprandial state, which also contributes to the idea that regulation of the production of apoB-containing lipoproteins in the intestine might be different from the liver.

Our results show fenofibrate to be an effective treatment for postprandial hyperlipidemia in CD36KO mice, and the reduction in the intestinal production of ApoB-containing lipoproteins as a new mechanism of action for this drug. Thus, since human CD36 deficiency is a genetic background of metabolic syndrome, as stated previously, we suggest that fenofibrate might play a similar role not only in CD36-deficient patients, but in MetS; this hypothesis, however, needs to be tested in further studies.

Conclusion

Fenofibrate reduces postprandial hypertriglyceridemia in CD36 knockout mice; this reduction is associated with the inhibition of intestinal apoB-48 production and the subsequent reduction of intestinal apoB-containing lipoproteins. This suggests a protective effect of fenofibrate against atherosclerosis in CD36KO mice as a monogenic model of metabolic syndrome.

Acknowledgments

This work was supported by the following grants: a grant-in-aid for Scientific Research (No. 18659267) to S. Yamashita from the Ministry of Education, Science, Sports and Culture in Japan; a grant from Mitsui Life Social Welfare Foundation to S. Yamashita; a Takeda Medical Research Foundation Grant to S. Yamashita.

References

1) Third report of the National Cholesterol Education Program (NCEP). Expert Panel on Detection, Evaluation and Treatment of High Blood cholesterol in Adults (Adult treatment panel III). Final report. Circulation, 2002; 106: 3163-3223
2) Carr D, Utzschneider K, Hull R, Kodama K, Retzlaff B, Brunzell J, Shofer J, Fish B, Knopp R, Kahn S: Intra-abdominal fat is a major determinant of the national cholesterol education program adult treatment panel III criteria for the metabolic syndrome. Diabetes, 2004; 53: 2087-2094
3) Alberti G: Introduction to the metabolic syndrome. Eur Heart J (Suppl), 2005; 7: D3-D5
4) Austin MA, Hokanson JE, Edwards KL: Hypertriglyceridemia as a cardiovascular risk factor. Am J Cardiol, 1998; 81: 7B-12B
5) Assmann G, Schulte H, Funke H, von Eckardstein A: The emergence of triglycerides as a significant independent risk factor in coronary artery disease. Eur Heart J, 1998; 19 (Suppl M): M8-M14
6) Nordestgaard B, Benn M, Schnohr P, Tybjærg-Hansen A: Nonfasting triglycerides and risk of myocardial infarction, ischemic heart disease, and death in men and women. JAMA, 2007; 298: 299-308
7) Bansal S, Buring JE, Rifai N, Mora S, Sacks FM, Ridker PM: Fasting compared with nonfasting triglycerides and risk of cardiovascular events in women. JAMA, 2007; 298: 309-316
8) Freiberg JJ, Tybjaerg-Hansen A, Jensen JS, Nordestgaard BG: Nonfasting triglycerides and risk of ischemic stroke in the general population. JAMA, 2008; 300: 2142-2152
9) Stalenhoef AF, de Graaf J: Association of fasting and nonfasting serum triglycerides with cardiovascular disease and the role of remnant-like lipoproteins and small dense LDL. Curr Opin Lipidol, 2008; 19: 355-361
10) Baillie AG, Coburn CT, Abumrad NA: Reversible binding of long-chain fatty acids to purified FAT, the adipose CD36 homolog. J Membr Biol, 1996; 153: 75-81
11) Su X, Abumrad NA: Cellular fatty acid uptake: A pathway under construction. Trends Endocrinol Metab, 2009; 20: 72-77
12) Kuwasako T, Hirano K, Sakai N, Ishigami M, Hiraoka H, Yakub MJ, Yamauchi-Takihara K, Yamashita S, Matsuzawa Y: Lipoprotein abnormalities in human genetic CD36 deficiency associated with insulin resistance and abnormal fatty acid metabolism. Diabetes Care, 2003; 26: 1647-1648
13) Yamashita S, Hirano K, Kuwasako T, Janabi M, Toyama Y, Ishigami M, Sakai N: Physiological and pathological roles of a multi-ligand receptor CD36 in atherogenesis; insights from CD36-deficient patients. Mol Cell Biochem, 2007; 299: 19-22
14) Goudriaan JR, den Boer MA, Rensen PC, Febbraio M, Kuipers F, Romijn JA, Havekes LM, Voshol PJ: CD36 deficiency in mice impairs lipoprotein lipase-mediated triglycerides clearance. J Lipid Res, 2005; 46: 2175-2181
15) Masuda D, Hirano K, Oku H, Sandoval JC, Kawase R, Yuasa-Kawase M, Yamashita Y, Takada M, Tsubakio-

Yamamoto K, Tochino Y, Koseki M, Matsuura F, Nishida M, Kawamoto T, Ishigami M, Hori M, Shimomura I, Yamashita S: Chylomicron remnants are increased in the postprandial state in CD36 deficiency. J Lipid Res, 2009; 50: 999-1011

16) Braissant O, Foufelle F, Scotto C, Dauca M, Wahli W: Differential expression of peroxisome proliferator activated receptors (PPARs): Tissue distribution of PPARα, β and γ in the adult rat. Endocrinology, 1996; 137: 354-366
17) Rosenson RS, Helenowski IW, Wolff DA, Rademaker AW, Huskin AL: Fenofibrate therapy ameliorates fasting and postprandial lipoproteinemia, oxidative stress, and the inflammatory response in subjects with hypertriglyceridemia and the metabolic syndrome. Diabetes Care, 2007; 30: 1945-1951
18) The FIELD study investigators: Effects of long-term fenofibrate therapy on cardiovascular events in 9795 people with type 2 diabetes mellitus (the FIELD study): randomized controlled trial. Lancet, 2005; 366: 1849-1861
19) Moore KJ, J El Khoury J, Medeiros LA, Terada K, Geula C, Luster AD, Freeman MW: A CD36-initiated signaling cascade mediates inflammatory effects of beta-amyloid. J Biol Chem, 2002; 277: 47373-47379
20) Okazaki M, Usui S, Fukui A, Kubota I, Tomoike H: Component analysis of HPLC profiles of unique lipoprotein subclass cholesterols for detection of coronary artery disease. Clin Chem, 2006; 52: 2049-2053
21) Bollman, JL, Cain JC, Grindlay JH: Techniques for the collection of lymph from the liver, small intestine, or thoracic duct of the rat. J Lab Clin Med, 1949; 33: 1349-1352
22) Schoonjans K, Peinado-Onsurbe J, Lefebvre AM, Heyman RA, Briggs M, Deeb S, Staels B, Auwerx J: PPARα and PPARγ activators direct a distinct tissue-specific transcriptional response via a PPRE in the lipoprotein lipase gene. EMBO J, 1996; 15: 5336-5348
23) Staels B, Dallongeville J, Auwerx J, Schoonjans K, Leitersdorf E, Fruchart JC: Mechanism of action of fibrates on lipid and lipoprotein metabolism. Circulation, 1998; 98: 2088-2093
24) Srivastava RA, Jahagirdar R, Azhar S, Sharma S, Bisgaier CL: Peroxisome proliferator-activated receptor-alpha selective ligand reduces adiposity, improves insulin sensitivity and inhibits atherosclerosis in LDL receptor-deficient mice. Mol Cell Biochem, 2006; 285: 35-50
25) Ginsberg HN, Fisher EA: The ever-expanding role of degradation in the regulation of apolipoprotein B metabolism. J Lipid Res, 2009; 50 Suppl: S162-166
26) Fu T, Mukhopadhyay D, Davidson NO, Borensztajn J: The peroxisome proliferators-activated receptor alpha (PPARalpha) agonist ciprofibrate inhibits apolipoprotein B mRNA editing in low density lipoprotein receptor-deficient mice: effects on plasma lipoproteins and the development of atherosclerotic lesions. J Biol Chem, 2004; 279: 28662-28669
27) Amèen C, Edvardsson U, Ljungberg A, Asp L, Akerblad P, Tuneld A, Olofsson SO, Lindén D, Oscarsson J: Activation of peroxisome proliferators-activated receptor alpha increases the expression and activity of microsomal triglyceride transfer protein in the liver. J Biol Chem, 2005; 280: 1224-1229

Journal of Molecular and Cellular Cardiology 49 (2010) 113–120

Contents lists available at ScienceDirect

Journal of Molecular and Cellular Cardiology

journal homepage: www.elsevier.com/locate/yjmcc

Original Article

ATF6 is important under both pathological and physiological states in the heart

Hauhiro Toko [a,1], Hidehisa Takahashi [a,1], Yosuke Kayama [a], Sho Okada [a], Tohru Minamino [a], Fumio Terasaki [c], Yasushi Kitaura [c], Issei Komuro [a,b,*]

[a] Department of Cardiovascular Science and Medicine, Chiba University Graduate School of Medicine, Chiba, Japan
[b] Department of Cardiovascular Medicine, Osaka University Graduate School of Medicine, Osaka, Japan
[c] Department of Internal Medicine III, Osaka Medical College, Takatsuki, Japan

ARTICLE INFO

Article history:
Received 5 November 2009
Received in revised form 25 March 2010
Accepted 26 March 2010
Available online 7 April 2010

Keywords:
ER stress
ATF6
AEBSF
Transgenic mice
Myocardial infarction
Dominant negative
Constitutively active
Apoptosis
Bcl-2

ABSTRACT

Accumulation of unfolded proteins in the endoplasmic reticulum (ER) evokes the ER stress response, including activating transcription factor 6 (ATF6), a key transcriptional activator to maintain cellular homeostasis. The ER stress has recently been reported to cause various diseases, but the role of ATF6 in the heart remains unknown. We clarified the role of ATF6 in the heart. The ATF6 activity was increased in the murine heart after myocardial infarction (MI). Treatment of mice with 4-(2-aminoethyl) benzenesulfonyl fluoride, an inhibitor of ATF6, further reduced cardiac function and increased the mortality rate at 14 days after MI. Pharmacological inhibition of ATF6 induced dilatation of left ventricle and depression of cardiac function even in sham-operated murine hearts. The transgenic mice that expressed dominant negative mutant of ATF6 showed larger left ventricular dimension and reduced fractional shortening compared with wild-type littermates, resulting in death of heart failure at ~8 weeks of age. In contrast, cardiac function after MI was better in transgenic mice that expressed constitutively active mutant of ATF6, compared with wild-type littermates. These results suggest that activation of the ER stress response factor ATF6 plays a critical role in not only protecting hearts under the pathological state but also maintaining cardiac function under the physiological state.

1. Introduction

Newly synthesized secretory and transmembrane proteins are folded and modified in the endoplasmic reticulum (ER). A variety of extracellular stresses such as nutrient deprivation, hypoxia, oxidative stress, and calcium depletion induce accumulation of unfolded proteins in the ER [1,2], triggering the ER stress response to prevent cell death by attenuation of protein synthesis, induction of ER chaperones, and promotion of ER-associated protein degradation (ERAD) [3–5]. The quality of protein folding is monitored by ER membrane proteins, PKR-like ER kinase (PERK), activating transcription factor 6 (ATF6), and inositol requirement 1 (IRE1). Failure of these adaptive responses causes cellular dysfunction and cell death, resulting in a wide range of human disorders such as neurodegenerative diseases, inflammation and diabetes [6,7]. Targeted disruption in intestinal epithelial cells of X-box binding protein 1 (XBP1) gene, a transcription factor which undergoes unconventional splicing mediated by IRE1, has been reported to cause spontaneous colitis [8]. Abnormal long polyglutamine expansions impair ERAD [9] and cause several neurodegenerative disorders, and disruption of SIL1, a cochaperone of glucose-regulated protein 78/binding immunoglobulin protein (BiP), causes the accumulation of protein aggregates and neurodegeneration [10]. In Akita diabetic mice, mRNA levels of BiP and C/EBP homologous protein (CHOP) are increased and deletion of CHOP delays the onset of diabetes [11]. PERK null mice exhibit pancreatic β cell death and develop diabetes [12]. Furthermore, ATF6 mutation observed in Pima Indians correlates with increased susceptibility to type 2 diabetes [13]. Although it has been reported that the ER stress is increased in hypertrophic hearts [14], the precise role of the ER stress response in the heart remains unclear.

We examined the role of the ER stress response in the heart, particularly focusing on ATF6. ATF6 is a transmembrane basic leucine zipper transcription factor. In the absence of the ER stress, BiP binds to the ER luminal domain of ATF6 and inhibits ATF6 translocation from the ER to the Golgi apparatus. When the ER stress is increased, BiP dissociates from ATF6, leading to translocation of ATF6 to the Golgi apparatus. In the Golgi apparatus, ATF6 is cleaved by site-1 and site-2 proteases, and the cytoplasmic N-terminal portion of ATF6, which has a DNA-binding domain and a transcriptional activation domain, translocates to the nucleus, and activates transcription of ER-related genes such as BiP [15,16].

In this study, we clarified the role of the ER stress in the heart by examining ATF6. ATF6 was activated in the murine heart after myocardial infarction (MI). Treatment of mice with AEBSF, an

* Corresponding author. Department of Cardiovascular Science and Medicine, Chiba University Graduate School of Medicine, 1-8-1 Inohana, Chuo-ku, Chiba 260-8670, Japan. Tel.: +81 43 226 2907; fax: +81 43 226 2557.
E-mail address: komuro-tky@umin.ac.jp (I. Komuro).
[1] Contributed equally to this paper.

0022-2828/$ – see front matter © 2010 Elsevier Ltd. All rights reserved.
doi:10.1016/j.yjmcc.2010.03.020

inhibitor of ATF6, impaired cardiac function and increased the mortality rate at 14 days after MI. Furthermore, in transgenic mice, which expressed dominant negative mutant of ATF6, left ventricle was dilated and cardiac function was worse than wild-type littermates. In contrast, cardiac function after MI was better in transgenic mice, which expressed constitutively active form of ATF6, compared with wild-type littermates. These results suggest that ATF6 plays a crucial role in not only protecting cardiac remodeling under the pathological state but also maintaining cardiac function under the physiological state.

2. Materials and methods

2.1. Mice and surgical procedures

All experimental procedures were performed according to the guidelines established by Chiba University for experiments in animals and all protocols were approved by our institutional review board. We generated transgenic mice that expressed constitutively active mutant or dominant negative mutant of ATF6 in the heart [17]. A HA tag was inserted at the amino terminus just distal to the translational start site of the mutated ATF6 cDNA. The mutated cDNA was subcloned into murine α-myosin heavy chain (α-MHC) promoter-containing expression vector. The linearized DNA was injected into pronuclei of eggs from C57BL6 mice, and the eggs were transferred into the oviducts of pseudopregnant ICR mice. The transgene was identified by PCR with transgene-specific primers and by Southern blot analysis. Generation and genotyping of transgenic mice with cardiac-restricted overexpression of human Bcl-2 have been previously described [18]. The strain of Bcl-2 transgenic was mix-background between FVBN and C57BL/6. The wild-type littermates were served as controls for all studies. We anesthetized mice by intraperitoneally injecting 50 mg/kg pentobarbital sodium. Myocardial infarction (MI) was produced by ligation of the left anterior descending artery. To inhibit activation of ATF6, 4-(2-aminoethyl) benzenesulfonyl fluoride (AEBSF, 4.8 μg/g/day, Sigma, Saint Louis, MO) was continuously administered by osmotic minipump (DURECT, Cupertino, CA).

2.2. Echocardiography

Cardiac function was examined by echocardiogram (Vevo 660, VISUAL SONICS, Ontario, Canada) provided with a 25-MHz imaging transducer. All recordings were performed on conscious mice.

2.3. Histology

Hearts fixed in 10% formalin were embedded in paraffin, sectioned at 4 μm thickness, and stained with hematoxylin and eosin. For electron microscopic analysis, hearts were fixed in 4% paraformaldehyde containing 0.25% glutaraldehyde, postfixed in 1% osmium tetroxide, and embedded in Epon 812. Ultrathin sections were stained with uranyl acetate and lead citrate. For detection of apoptotic cells, TUNEL labeling was performed with an In Situ Apoptosis Detection kit (Takara, Shiga, Japan). We counted the numbers of TUNEL-positive cardiomyocytes and hematoxylin-stained nuclei in a whole section of each samples. To analyze the number of apoptotic cells in infarcted hearts, digital photographs were taken at magnification ×200, and 20 random high-power fields (HPF) from each heart samples were chosen and quantified in a blinded manner.

2.4. Western blot analysis

Whole cell lysates were resolved by SDS-polyacrylamide gel electrophoresis. Proteins were transferred onto a nitrocellulose transfer membrane (Whatman, Dassel, Germany). Western blot analysis was performed with antibodies against HA (Santa Cruz Biotechnology, Santa Cruz, CA), ATF6 (IMGENEX, San Diego, CA), BiP (Stressgen Bioreagents, Victoria, Canada), or actin (Sigma). Hybridizing bands were visualized using an ECL detection kit (GE Healthcare, Buckinghamshire, UK).

2.5. Cell culture

Cardiomyocytes were prepared from ventricles of 1-day-old Wistar rats and cultured in Dulbecco's modified Eagle's medium supplemented with 10% fetal bovine serum at 37 °C in a mixture of 95% air and 5% CO_2. Cardiomyocytes were exposed to $CoCl_2$ (100 μM, Sigma) with or without AEBSF (300 μM) for 24 h. HEK293 cells were transfected with an expression plasmid encoding mutant form of ATF6 using FuGENE6 (Roche, Indianapolis, IN). The HEK293 cells were exposed to tunicamycin (TM, 2 μg/mL, Sigma) for 6 h.

2.6. RNA extraction and quantitative RT-PCR analysis

Total RNA was isolated from the heart, neonatal cardiomyocytes or HEK293 cells with RNAZol-B (Molecular Research Center, Cincinnati, OH) according to the manufacturer's instructions. cDNA synthesis of 1 μg of RNA was carried out by using QuantiTect Reverse Transcription Kit (QIAGEN, Hilden, Germany). Quantitative real time (RT)-PCR was performed by using the LightCycler with Taqman Universal Probe Library and the Light Cycler Master (Roche).

2.7. Immunohistochemistry

Cardiomyocytes of neonatal rats cultured on glass cover slips were incubated with the antibody to α-actinin (Sigma), followed by incubation with Cy3-labeled secondary antibodies. Nuclei were counterstained with Hoechst 33258 dye. An antibody against HA was incubated with the paraffin sections of murine hearts, and immunoreactivity was evaluated using the avidin–biotin–peroxidase complex method (ScyTek Laboratories, Logan, UT). The reactions were optimized using diaminobenzidine chromogen (Vector Laboratories, Burlingame, CA) and were counterstained with hematoxylin.

2.8. Statistical analysis

Data are shown as mean ± s.e.m. Multiple group comparison was performed by one-way analysis of variance (ANOVA) followed by the Bonferroni procedure for comparison of means. Comparisons between two groups were analyzed by the two-tailed Student's *t*-test. Values of $P<0.05$ were considered statistically significant.

3. Results

3.1. ER stress response in the ischemic heart

To elucidate whether the ER stress is increased in the heart under stress conditions, we produced MI in wild-type mice. The mRNA and protein levels of BiP were increased from 1 to 4 days after MI, respectively (Fig. 1a and b). The protein levels of total (90 kDa, p90ATF6) and cleaved form (50 kDa, p50ATF6) of ATF6 and the mRNA levels of ATF6 were increased after MI (Fig. 1a and b). Furthermore, phosphorylation levels of PERK and its target protein eukaryotic initiation factor (eIF) 2α were increased at 1 and 4 days after MI, respectively (Supplemental Fig. 1a). Although phosphorylation levels of IRE1 were not significantly increased, levels of its activated form XBP1 were increased (Supplemental Fig. 1a and b). The mRNA levels of CHOP were also increased (Fig. 1b). CHOP is a transcription factor that regulates apoptosis-related factors under the ER stress condition. These results suggest that the ER stress response is induced in the heart after MI.

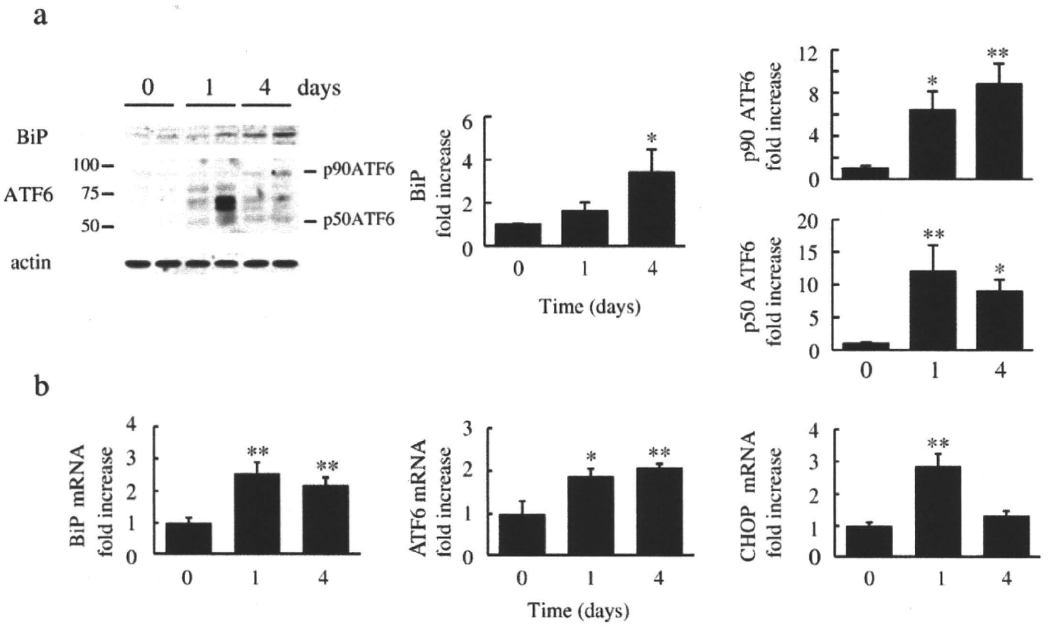

Fig. 1. ER stress response occurs in the ischemic heart. (a) Infarcted hearts during 4 days were analyzed for protein levels of BiP and total (p90ATF6) and cleaved form (p50ATF6) of ATF6 by Western blot analysis. Molecular mass makers (kDa) are indicated on the left. Quantification of BiP and ATF6 proteins as compared with sham (time = 0). *$P<0.05$, **$P<0.01$ versus day 0. $n=4$. (b) Expression levels of BiP, ATF6 and CHOP in hearts during 4 days of MI were quantified by RT-PCR analysis, normalized against GAPDH mRNA expression. *$P<0.05$, **$P<0.01$ versus day 0. $n=5$.

3.2. Inhibition of ATF6 in the ischemic heart

We examined the role of ATF6 in the ischemic heart using AEBSF, an ATF6 inhibitor [19]. We treated wild-type mice with AEBSF or vehicle and produced MI. The treatment with AEBSF was effective because it inhibited the cleavage of ATF6 (p50ATF6) in the ischemic heart (Fig. 2a). The survival rate after MI was much lower in mice treated with AEBSF than in mice treated with vehicle (Fig. 2b). In echocardiography, left ventricular posterior wall thickness was thinner, left ventricular dimension was larger and fractional shortening was smaller in mice treated with AEBSF than in mice treated with vehicle at 14 days after MI (Fig. 2c, Supplemental Table 1). These results suggest that ATF6 prevents cardiac remodeling after MI.

To clarify how AEBSF enhanced cardiac remodeling after MI, we examined expression levels of BiP, an ER chaperone which is induced by ATF6 and helps to refold unfolding proteins and ameliorates the ER stress [3,20]. mRNA levels of BiP were decreased in hearts by the treatment with AEBSF (Fig. 3a). Since it has been reported that overwhelming of the ER stress induces apoptosis, we examined apoptosis by TUNEL method. The number of TUNEL-positive cells was greater in AEBSF-treated group than in vehicle-treated group at 24 h after MI (Fig. 3b). Furthermore, expression level of CHOP was more strongly increased in AEBSF-treated group after MI (Fig. 3c). We exposed cultured cardiomyocytes to $CoCl_2$, a hypoxia mimetic, with or without AEBSF for 24 h. AEBSF augmented $CoCl_2$-induced cardiomyocyte apoptosis (Fig. 3d). To further clarify the role of ATF6 in cardiomyocytes under ischemic condition, we used a siRNA against rat ATF6. The siRNA decreased expression level of ATF6 in cardiomyocytes (Supplemental Fig. 2a), and augmented cardiomyocyte apoptosis (Supplemental Fig. 2b, lane 1 versus lane 3 and lane 5 versus lane 7). Next, we examined whether off target effects of AEBSF affect cardiomyocyte death. In the presence of the siRNA, AEBSF further increased the number of cardiomyocyte death (Supplemental Fig. 2b, lane 3 versus lane 4, lane 7 versus lane 8), suggesting that the effect of AEBSF on the heart is not only ATF6 inhibition but also some additional effects. These results suggest that inhibition of ATF6 increases ER stress-induced apoptotic death of cardiomyocytes in the ischemic heart, resulting in enhancement of cardiac remodeling after MI.

3.3. Role of dominant negative mutant of ATF6 in the heart

Pharmacological inhibition of ATF6 with AEBSF induced dilatation of left ventricle and depression of cardiac function even in sham-operated murine hearts (Fig. 2c), suggesting that ATF6 also plays a critical role in maintaining cardiac homeostasis under the physiological state. There are two forms of ATF6, ATF6α and ATF6β [21]. It has been reported that knockout mice of either ATF6α or ATF6β does not show significant phenotypes, while their double knockout mice are embryonic lethal [22,23]. Therefore, to define the role of ATF6 in the heart under the physiological state, we made transgenic mice (dnTg) that expressed a dominant negative mutant of ATF6 with HA tag under the control of α-MHC promoter (Fig. 4a) [17]. The dominant negative mutant of ATF6 has only a cytoplasmic domain of ATF6 and amino acids 315–317 of the cytoplasmic domain are changed from KNR to TAA. It has been reported that the mutant would be predicted to disrupt DNA-binding activity but dimerize with endogenous ATF6 and prevent its binding to ATF6 DNA-binding sites [17]. To confirm the effect of the mutant, we examined the expression levels of BiP in HEK293 cells transfected with the mutant. The mutant attenuated the increase of BiP expression levels by treatment of tunicamycin (TM), an ER stress inducer (Fig. 4b). Western blot analysis showed that HA was detected only in hearts of dnTg mice, and immunohistochemical analysis showed that the mutant was expressed at the nucleus of cardiomyocytes in dnTg mice (Fig. 4c). To examine whether the mutant acts as a dominant negative in vivo, we performed quantitative RT-PCR of ATF6-target genes such as BiP and ER degradation enhancing like protein 1 (EDEM1) [20,23]. The mRNA levels of BiP and EDEM1 were lower in hearts of dnTg mice compared with wild-type littermates (Fig. 4d). The survival rate was significantly lower in dnTg mice than wild-type littermates (Fig. 4e). The wall of left ventricle was thin and the cavity of hearts was dilated in dnTg mice (Fig. 4f). Echocardiographic analysis showed that left ventricular posterior wall thickness was thinner, left ventricular

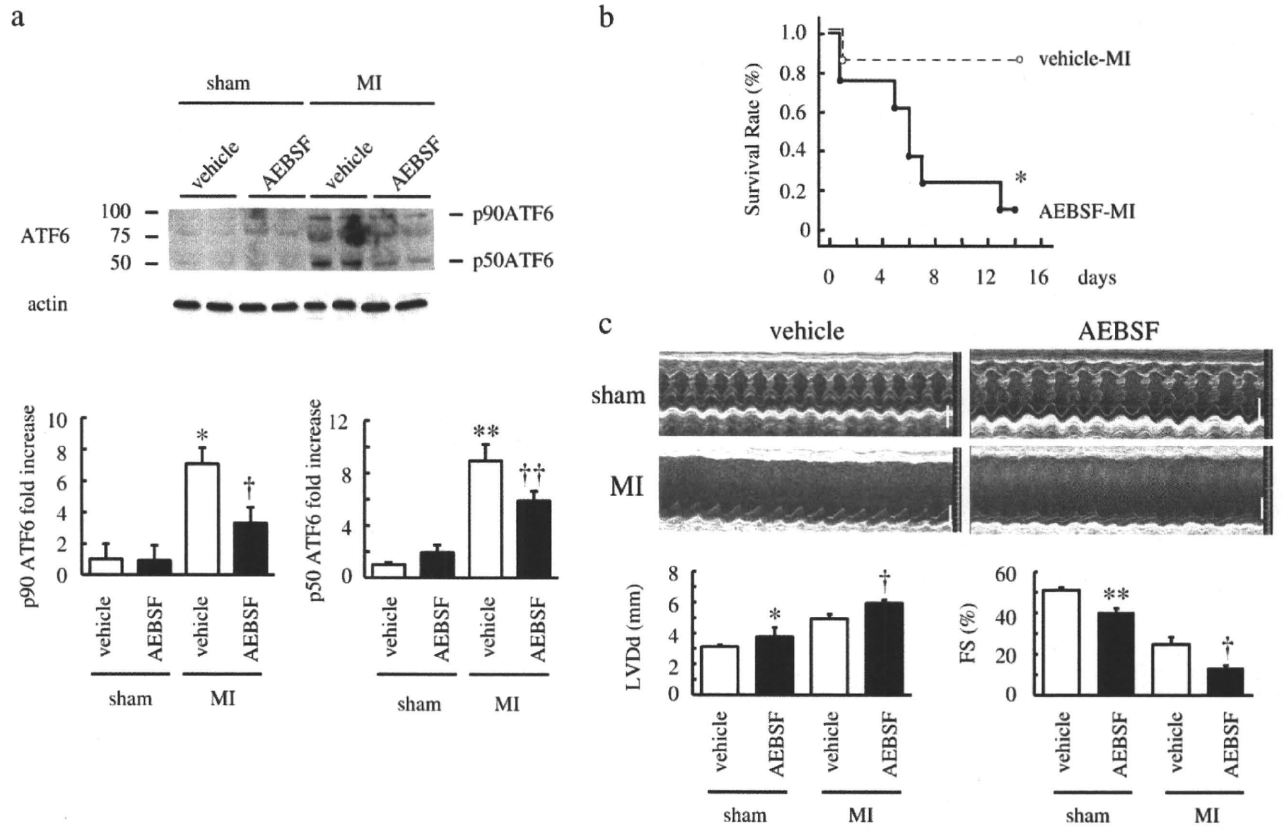

Fig. 2. AEBSF enhances cardiac remodeling after MI. (a) Sham-operated or infarcted hearts treated with vehicle or AEBSF were analyzed for protein levels of total (p90ATF6) and cleaved form (p50ATF6) of ATF6 by western blot analysis. Molecular mass makers (kDa) are indicated on the left. Quantification of ATF6 proteins as compared with sham-vehicle group. **P*<0.05, ***P*<0.01 versus sham treated with vehicle. †*P*<0.05, ††*P*<0.01 versus MI treated with vehicle. *n* = 4. (b) Kaplan–Meier survival curve after MI. **P*<0.05 versus MI treated with vehicle. Vehicle, *n* = 10; AEBSF, *n* = 23. (c) Left ventricular end-diastolic dimension (LVDd) and fractional shortening (FS) were examined at 14 days after MI by echocardiogram. Scale bar, 2 mm. **P*<0.05, ***P*<0.01 versus sham treated with vehicle. *P*<0.01 versus MI treated with vehicle.

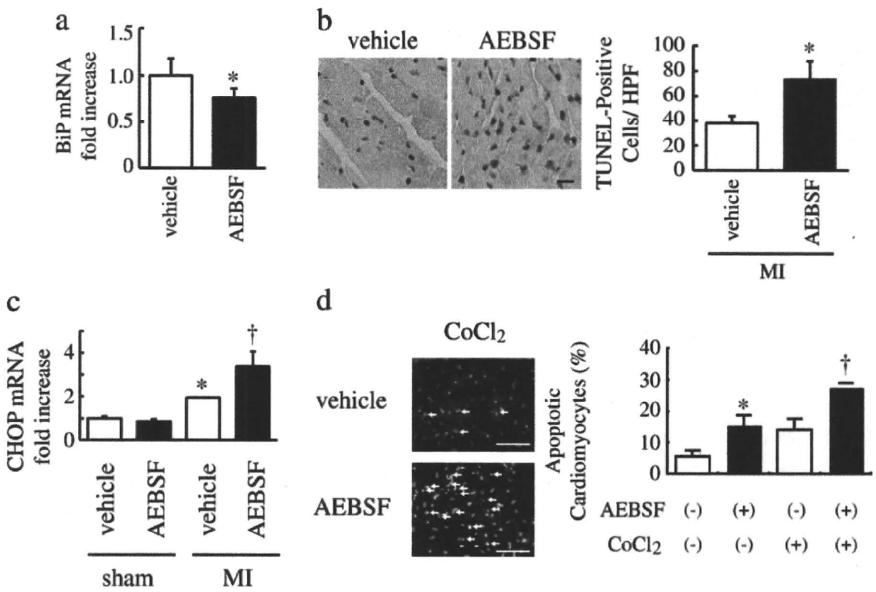

Fig. 3. AEBSF increases apoptotic cardiomyocytes. (a) Expression levels of BiP in sham-operated hearts were quantified by RT-PCR analysis, normalized against GAPDH mRNA expression. **P*<0.05 versus vehicle. *n* = 5. (b) TUNEL-positive cells (brown) in hearts at 24 h after MI. Scale bar, 10 μm. Quantitative analysis for TUNEL-positive cells at 24 h after MI. **P*<0.01 versus vehicle. *n* = 4. (c) Expression levels of CHOP in hearts of mice subjected with MI were quantified by RT-PCR analysis, normalized against GAPDH mRNA expression. **P*<0.05 versus sham treated with vehicle. †*P*<0.01 versus MI treated with vehicle. *n* = 5. (d) Cardiomyocytes were incubated with α-actinin (red), and nuclei were counterstained with Hoechst 33258 (blue). Arrows indicate condensed and Hoechst-stained nuclei indicative of apoptosis. The graph showed quantitative analysis for $CoCl_2$-induced apoptotic cardiomyocytes treated with vehicle or AEBSF. **P*<0.05 versus non-treated cardiomyocytes. †*P*<0.01 versus $CoCl_2$-treated cardiomyocytes with vehicle. *n* = 5. Scale bar, 100 μm.

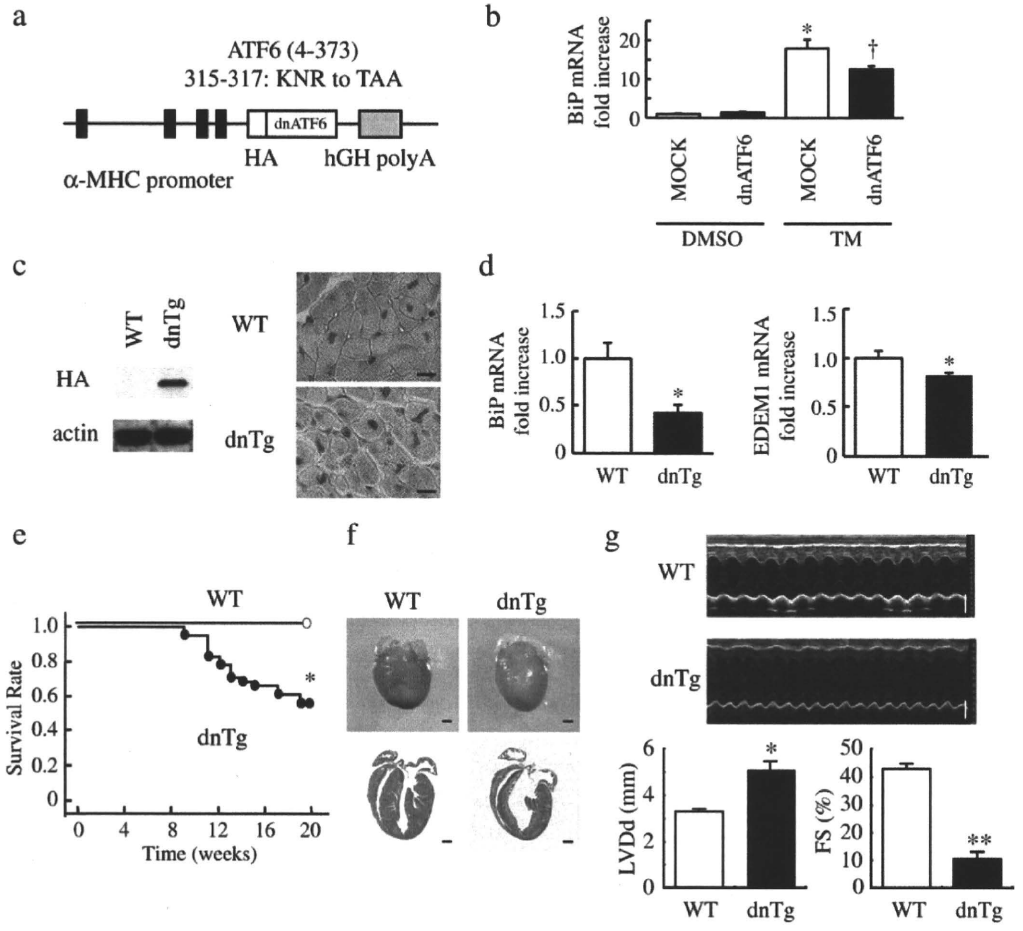

Fig. 4. The dominant negative mutant of ATF6 transgenic mice. (a) Schematic diagram represented the dominant negative mutant of ATF6 (dnATF6) transgene. HA-tagged dnATF6 was subcloned between the murine α-MHC promoter and human growth hormone (hGH) polyA. (b) Expression levels of BiP in HEK293 cells transfected with MOCK or an expression plasmid encoding the dominant negative mutant form of ATF6 were quantified by RT-PCR analysis, normalized against GAPDH mRNA expression. HEK293 cells were incubated with DMSO or TM for 6 h. *$P<0.01$ versus MOCK with DMSO, †$P<0.05$ versus MOCK with TM. $n=4$. (c) Western blot analysis and immunohistochemical staining (brown) for HA in hearts of wild-type littermates (WT) or dnTg mice at 8 weeks of age. Scale bar, 10 μm. (d) Expression levels of BiP and EDEM1 in hearts of WT or dnTg mice at 8 weeks of age were quantified by RT-PCR analysis, normalized against GAPDH mRNA expression. *$P<0.05$ versus WT. $n=4$. (e) Kaplan–Meier survival curve. *$P<0.05$ versus WT. WT, $n=19$; dnTg, $n=17$. (f) Gross morphology (upper images) and sections (lower images) of WT or dnTg murine hearts at 8 weeks of age. Scale bar, 1 mm. (g) Left ventricular end-diastolic dimension (LVDd) and fractional shortening (FS) were examined at 8 weeks of age by echocardiogram. Scale bar, 2 mm. *$P<0.05$, **$P<0.01$ versus WT.

dimension was larger and systolic function was impaired in dnTg mice compared with those in wild-type littermates (Fig. 4g, Supplemental Table 2). These results suggest that ATF6 is necessary to maintain cardiac function and structure under the physiological state.

Electron microscopic analysis showed that endoplasmic reticulums were expanded (Fig. 5a, 3 and I) and myofilaments were decreased (Fig. 5a, 4 and II) in cardiomyocytes of dnTg mice compared with wild-type littermates (Fig. 5a, 1 and 2). Expanded endoplasmic reticulums indicated that the ER stress was increased. Degenerated cardiomyocytes, suggesting apoptotic cardiomyocytes, were also observed in dnTg mice (Fig. 5a, 5 and III). Much more TUNEL-positive cardiomyocytes were observed in dnTg mice than in wild-type littermates (Fig. 5b). Furthermore, quantitative RT-PCR revealed that mRNA levels of ER stress-related apoptotic factors such as CHOP and p53 up-regulated modulator of apoptosis (PUMA) were upregulated in hearts of dnTg mice (Fig. 5c) [24,25]. To elucidate the role of cardiomyocyte apoptosis, we crossed dnTg mice and transgenic mice which overexpressed an anti-apoptotic protein Bcl-2 in cardiomyocytes [18]. Overexpression of Bcl-2 ameliorated dilatation of left ventricle and decrease of cardiac function (Fig. 5d, Supplemental Table 3), suggesting that ATF6 plays an important role in maintaining cardiac function and structure under the physiological state at least in part via inhibiting apoptosis of cardiomyocytes.

3.4. Role of constitutively active mutant of ATF6 in the heart

We next examined whether activation of ATF6 had protective effects on left ventricular remodeling after MI. Since only a cytoplasmic domain of ATF6 (aa1–373) activated expression of BiP gene (Fig. 6a) [16], we used this deletion mutant of ATF6 as a constitutively active form of ATF6. We generated transgenic mice (caTg) that expressed the cytoplasmic domain of ATF6 with HA tag under the control of α-MHC promoter (Fig. 6b) [17]. Western blot analysis showed that HA was detected only in hearts of caTg mice, and immunohistochemical analysis showed that the transgene was expressed at the nucleus of cardiomyocytes in caTg mice (Fig. 6c). There was no significant difference in heart size and cardiac function (Fig. 6d and e, Supplemental Table 4), suggesting that activation of ATF6 does not affect cardiac structure and function under the physiological state.

To examine whether activation of ATF6 had protective effects on the heart under the pathological state, we made MI in caTg mice. Echocardiographic study showed that left ventricular dimension was smaller and fractional shortening was better in caTg mice compared with in wild-type littermates at 14 days after MI (Fig. 6f). The number of TUNEL-positive cells was less in hearts of caTg mice than wild-type littermates at 24 h after MI (Fig. 6g). The survival rate was better in caTg

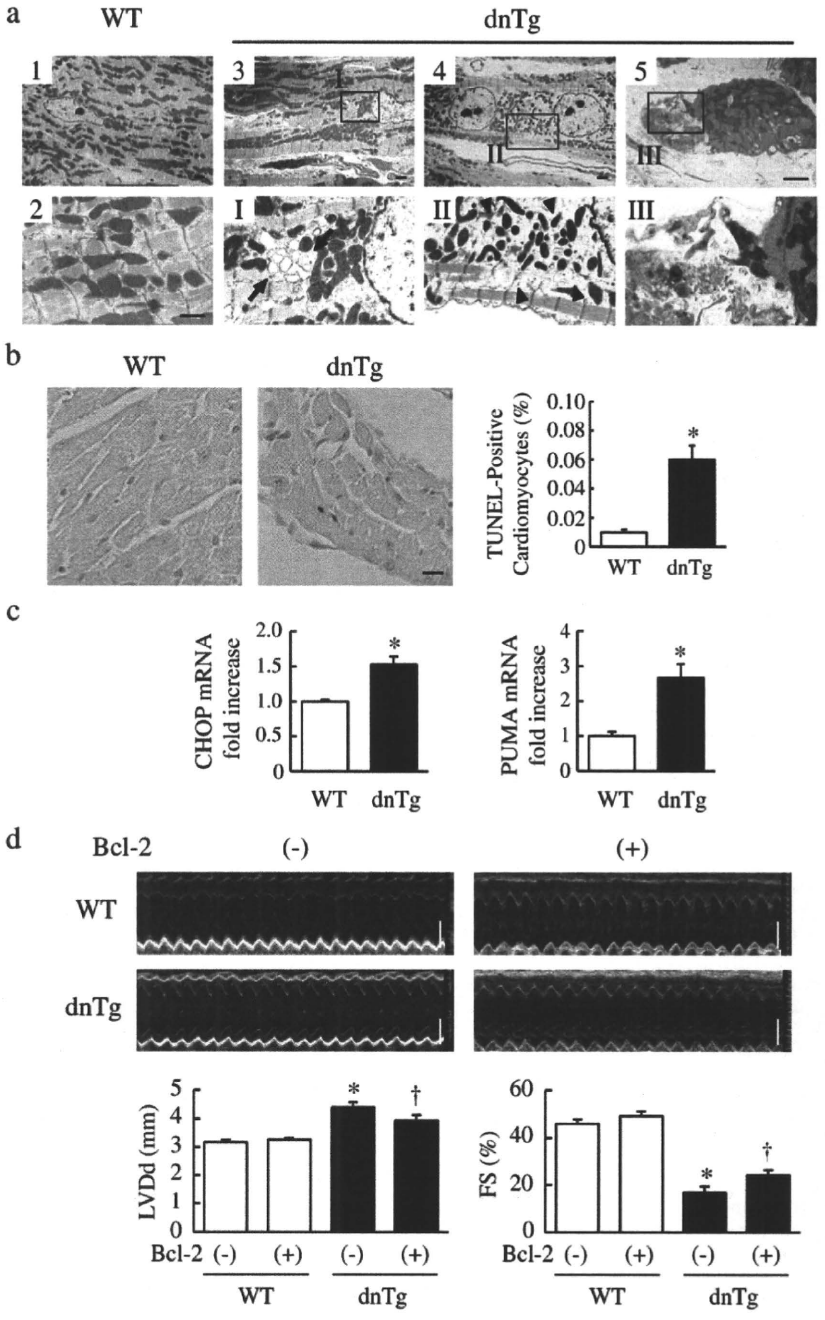

Fig. 5. Apoptotic cardiomyocytes are increased in dominant negative mutant of ATF6 transgenic mice. (a) Electron microscopic analysis. Endcoplasmic reticulums were expanded (arrow, 3 and I) and myofilaments were decreased (arrow head, 4 and II) in cardiomyocytes of dnTg mice. Degenerated cardiomyocytes were observed in dnTg mice (5 and III). Scale bar, 1 μm. WT, wild-type littermates. (b) TUNEL-positive cardiomyocytes (brown) in hearts of WT or dnTg mice. Scale bar, 10 μm. The graph showed quantitative analysis for TUNEL-positive cardiomyocytes at 8 weeks of age. *$P<0.05$ versus WT. $n=5$. Scale bar, 10 μm. (c) Expression levels of CHOP and PUMA in hearts of WT or dnTg mice were quantified by RT-PCR analysis, normalized against GAPDH mRNA expression. *$P<0.05$ versus WT. $n=4$. (d) Left ventricular end-diastolic dimension (LVDd) and fractional shortening (FS) were examined at 8 weeks of age by echocardiogram. Scale bar, 2 mm. *$P<0.01$ versus WT Bcl-2(−) mice, †$P<0.05$ versus dnTg Bcl-2(−) mice.

mice than in wild-type littermates even when they were treated with AEBSF (Supplemental Fig. 3a). On the other hand, the survival rate was lower in dnTg mice than in wild-type littermates (Supplemental Fig. 3b). These results suggest that activation of ATF6 has protective effects on cardiomyocytes and prevents cardiac remodeling after MI.

4. Discussion

Recent reports show that the ER stress response is activated in the heart exposed to prolonged stresses such as pressure overload [14] as well as acute stresses such as ischemia/reperfusion [26]. Although there is a report showing that BiP expression is detected in cardiomyocytes of border zone after MI [27], expressions of other ER stress-related factors are not known in hearts after MI. We revealed that all three branches of ER stress sensor, such as ATF6, PERK, and IRE1, were activated in the MI heart (Fig. 1, Supplemental Fig. 1). The mRNA and protein levels of an ER chaperone BiP, which is regulated by ATF6, were also increased (Fig. 1). Furthermore, the mRNA levels of CHOP were increased, which has been reported to induce apoptosis under excessive ER stress (Fig. 1b). These results suggest that the ER stress response is induced in the heart by MI and that excessive ER stress induces apoptosis of cardiomyocytes after MI.

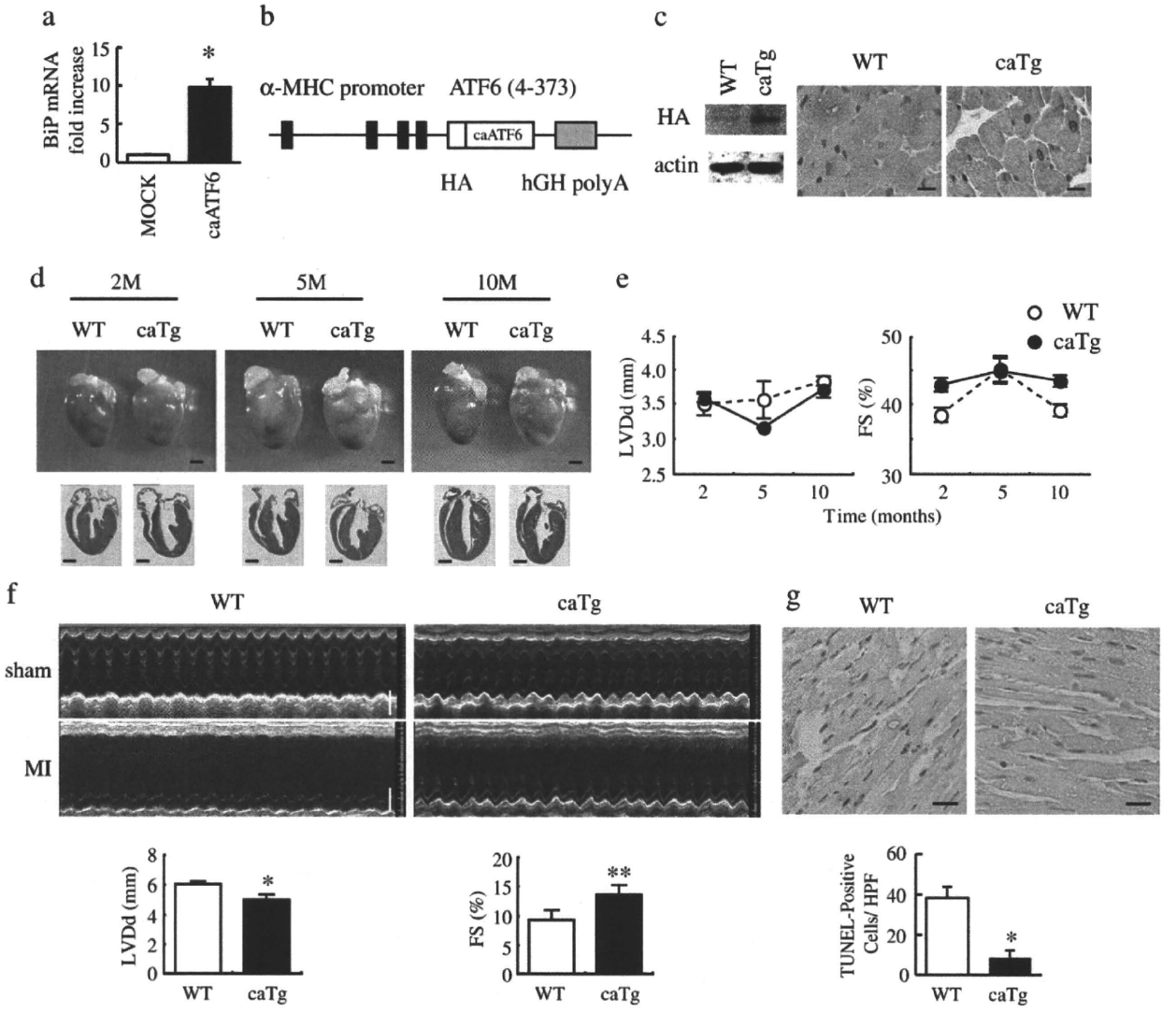

Fig. 6. The constitutively active mutant of ATF6 transgenic mice. (a) Expression levels of BiP in HEK293 cells transfected with MOCK or an expression plasmid encoding the constitutively active form of ATF6 were quantified by RT-PCR analysis, normalized against GAPDH mRNA expression. *$P<0.05$ versus MOCK. (b) Schematic diagram represented the constitutively active mutant of ATF6 (caATF6) transgene. HA-tagged caATF6 was subcloned between the murine α-MHC promoter and human growth hormone (hGH) polyA. (c) Western blot analysis and immunohistochemical staining (brown) for HA in hearts of wild-type littermates (WT) or caTg mice at 2 months of age. Scale bar, 10 μm. (d) Gross morphology (upper images) and sections (lower images) of WT or caTg murine hearts at 2, 5 and 10 months (M) of age. Scale bar, 1 mm. (e) Left ventricular end-diastolic dimension (LVDd) and fractional shortening (FS) were examined at 2, 5 and 10 months of age by echocardiogram. (f) Left ventricular end-diastolic dimension (LVDd) and fractional shortening (FS) were examined at 14 days after myocardial infarction by echocardiogram. Scale bar, 2 mm. *$P<0.05$, **$P<0.01$ versus WT. (g) TUNEL-positive cells (brown) in hearts at 24 h after MI. Scale bar, 10 μm. The graph showed quantitative analysis for TUNEL-positive cells at 24 h after MI. Scale bar, 100 μm. *$P<0.05$ versus vehicle. $n=3$.

ATF6 is a major transcription factor to induce gene expression of ER chaperones as well as ERAD components [22]. We firstly produced MI in wild-type mice in the presence of an ATF6 inhibitor, AEBSF. AEBSF has been reported to inhibit site-1 protease in vitro, which cleaves and activates ATF6 [19]. In this study, AEBSF inhibited an increase of activated forms of ATF6 (p50ATF6) after MI (Fig. 2a), suggesting that AEBSF indeed suppressed ATF6 function also in vivo. AEBSF reduced survival rate and worsened cardiac function after MI (Fig. 2b and c, Supplemental Table 1). Although it remains unclear how inhibition of ATF6 function deteriorated cardiac remodeling after MI, suppression of BiP might be one reason (Fig. 3a). BiP is a chaperone to reduce the ER stress, and a recent report shows that BiP has protective effects on cardiomyocytes against ischemic injury [28]. On the other hand, BiP null mice exhibit embryonic lethality because of an increase of apoptosis in the inner cell mass [29]. Suppression of BiP by AEBSF might increase apoptosis in the ischemic heart due to excessive ER stress, resulting in deterioration of cardiac remodeling. Indeed, the number of TUNEL-positive cells and expression level of CHOP were increased more in the MI heart by AEBSF treatment (Fig. 3b and c). The in vitro result that the number of CoCl2-induced apoptotic cardiomyocytes was increased more by AEBSF further supports this idea (Fig. 3day).

Targeted disruption of XBP1 gene is embryonic lethal in mice because of cardiac developmental defects [30]. Double knockout mice of ATF6α and ATF6β gene are also embryonic lethal [22]. On the other hand, PERK knockout mice exhibit death of pancreatic β cells and develop diabetes [12]. Although these studies suggest that the ER stress response is important for development and homeostasis of organs, the physiological role of the ER stress response in the heart has not been fully elucidated. To clarify the role of the ER stress response, especially ATF6 in the heart under physiological state, we established mice that expressed dominant negative mutant of ATF6 in the heart (Fig. 4a). Heart size was enlarged and cardiac function was impaired in dnTg mice even without pathological stresses (Fig. 4f and g, Supplemental Table 2), suggesting that ATF6 is necessary to maintain cardiac structure and function in adulthood.

Electron microscopic analysis showed that endoplasmic reticulum was expanded in cardiomyocytes of dnTg mice (Fig. 5a), suggesting that the ER stress is increased. The number of TUNEL-positive cardiomyocytes was increased (Fig. 5b) and mRNA levels of ER stress-induced apoptosis-related genes such as CHOP and PUMA were upregulated in the heart of dnTg mice (Fig. 5c). Impaired ER stress response by dominant negative mutant of ATF6 might increase apoptotic cardiomyocytes even under physiological state, resulting in cardiac dysfunction. This idea was supported by the result that overexpression of Bcl-2 significantly improved cardiac function in dnTg mice (Fig. 5d, Supplemental Table 3).

Cardiac remodeling after MI was prevented in caTg mice (Fig. 6f, Supplemental Table 5), and was deteriorated in dnTg mice (Supplementary Fig. 2b). Furthermore, the reduced survival rate with AEBSF was improved in caTg mice (Supplemental Fig. 2a). These results suggest that ATF6 activation after MI is protective in the heart, which is consistent with the recent result of ischemia/reperfusion injury in hearts [26]. Although the decrease of TUNEL-positive cells might be involved in the prevention of cardiac remodeling after MI (Fig. 6g), precise mechanisms of how overexpression of ATF6 ameliorates cardiac remodeling remain to be determined.

This study indicates that activation of the ER stress response factor ATF6 plays a critical role in protecting hearts under the pathological state and maintaining cardiac function under the physiological state.

Acknowledgment

We thank R. Prywes (Columbia University, New York, NY) for a constitutively active and dominant negative mutants of ATF6 expression construct, M.D. Schneider (Imperial College, London, UK) for Bcl-2 transgenic mice and J. Robbins (Children's Hospital Research Foundation, Cincinnati, OH) for a fragment of α-MHC gene promoter. We thank E. Fujita, R. Kobayashi, Y. Ishiyama, I. Sakamoto, M. Ikeda, A. Furuyama and Y. Ohtsuki for technical support and M. Iiyama, K. Matsumoto, Y. Ishikawa and Y. Yasukawa for animal care.

Funding Sources: This work was supported by a Grant-in-Aid for Scientific Research on Priority Area and for Exploratory Research, Ministry of Education, Culture, Sports, Science and Technology (to I.K.).

Appendix A. Supplementary data

Supplementary data associated with this article can be found, in the online version, at doi:10.1016/j.yjmcc.2010.03.020.

References

[1] Frand AR, Cuozzo JW, Kaiser CA. Pathways for protein disulphide bond formation. Trends Cell Biol 2000;10:203–10.
[2] Gotoh T, Mori M. Nitric oxide and endoplasmic reticulum stress. Arterioscler Thromb Vasc Biol 2006;26:1439–46.
[3] Sitia R, Braakman I. Quality control in the endoplasmic reticulum protein factory. Nature 2003;426:891–4.
[4] Harding HP, Zhang Y, Ron D. Protein translation and folding are coupled by an endoplasmic-reticulum-resident kinase. Nature 1999;397:271–4.
[5] Brodsky JL, McCracken AA. ER protein quality control and proteasome-mediated protein degradation. Semin Cell Dev Biol 1999;10:507–13.
[6] Yoshida H. ER stress and diseases. FEBS J 2007;274:630–58.
[7] Kim R, Emi M, Tanabe K, Murakami S. Role of the unfolded protein response in cell death. Apoptosis 2006;11:5–13.
[8] Kaser A, Lee AH, Franke A, Glickman JN, Zeissig S, Tilg H, et al. XBP1 links ER stress to intestinal inflammation and confers genetic risk for human inflammatory bowel disease. Cell 2008;134:743–56.
[9] Duennwald ML, Lindquist S. Impaired ERAD and ER stress are early and specific events in polyglutamine toxicity. Genes Dev 2008;22:3308–19.
[10] Zhao L, Longo-Guess C, Harris BS, Lee JW, Ackerman SL. Protein accumulation and neurodegeneration in the woozy mutant mouse is caused by disruption of SIL1, a cochaperone of BiP. Nat Genet 2005;37:974–9.
[11] Oyadomari S, Koizumi A, Takeda K, Gotoh T, Akira S, Araki E, et al. Targeted disruption of the Chop gene delays endoplasmic reticulum stress-mediated diabetes. J Clin Invest 2002;109:525–32.
[12] Harding HP, Zeng H, Zhang Y, Jungries R, Chung P, Plesken H, et al. Diabetes mellitus and exocrine pancreatic dysfunction in perk-/- mice reveals a role for translational control in secretory cell survival. Mol Cell 2001;7:1153–63.
[13] Thameem F, Farook VS, Bogardus C, Prochazka M. Association of amino acid variants in the activating transcription factor 6 gene (ATF6) on 1q21-q23 with type 2 diabetes in Pima Indians. Diabetes 2006;55:839–42.
[14] Okada K, Minamino T, Tsukamoto Y, Liao Y, Tsukamoto O, Takashima S, et al. Prolonged endoplasmic reticulum stress in hypertrophic and failing heart after aortic constriction: possible contribution of endoplasmic reticulum stress to cardiac myocyte apoptosis. Circulation 2004;110:705–12.
[15] Shen J, Prywes R. ER stress signaling by regulated proteolysis of ATF6. Methods 2005;35:382–9.
[16] Haze K, Yoshida H, Yanagi H, Yura T, Mori K. Mammalian transcription factor ATF6 is synthesized as a transmembrane protein and activated by proteolysis in response to endoplasmic reticulum stress. Mol Biol Cell 1999;10:3787–99.
[17] Wang Y, Shen J, Arenzana N, Tirasophon W, Kaufman RJ, Prywes R. Activation of ATF6 and an ATF6 DNA binding site by the endoplasmic reticulum stress response. J Biol Chem 2000;275:27013–20.
[18] Tanaka M, Nakae S, Terry RD, Mokhtari GK, Gunawan F, Balsam LB, et al. Cardiomyocyte-specific Bcl-2 overexpression attenuates ischemia-reperfusion injury, immune response during acute rejection, and graft coronary artery disease. Blood 2004;104:3789–96.
[19] Okada T, Haze K, Nadanaka S, Yoshida H, Seidah NG, Hirano Y, et al. A serine protease inhibitor prevents endoplasmic reticulum stress-induced cleavage but not transport of the membrane-bound transcription factor ATF6. J Biol Chem 2003;278:31024–32.
[20] Adachi Y, Yamamoto K, Okada T, Yoshida H, Harada A, Mori K. ATF6 is a transcription factor specializing in the regulation of quality control proteins in the endoplasmic reticulum. Cell Struct Funct 2008;33:75–89.
[21] Haze K, Okada T, Yoshida H, Yanagi H, Yura T, Negishi M, et al. Identification of the G13 (cAMP-response-element-binding protein-related protein) gene product related to activating transcription factor 6 as a transcriptional activator of the mammalian unfolded protein response. Biochem J 2001;355:19–28.
[22] Yamamoto K, Sato T, Matsui T, Sato M, Okada T, Yoshida H, et al. Transcriptional induction of mammalian ER quality control proteins is mediated by single or combined action of ATF6alpha and XBP1. Dev Cell 2007;13:365–76.
[23] Wu J, Rutkowski DT, Dubois M, Swathirajan J, Saunders T, Wang J, et al. ATF6alpha optimizes long-term endoplasmic reticulum function to protect cells from chronic stress. Dev Cell 2007;13:351–64.
[24] Oyadomari S, Mori M. Roles of CHOP/GADD153 in endoplasmic reticulum stress. Cell Death Differ 2004;11:381–9.
[25] Nickson P, Toth A, Erhardt P. PUMA is critical for neonatal cardiomyocyte apoptosis induced by endoplasmic reticulum stress. Cardiovasc Res 2007;73:48–56.
[26] Martindale JJ, Fernandez R, Thuerauf D, Whittaker R, Gude N, Sussman MA, et al. Endoplasmic reticulum stress gene induction and protection from ischemia/reperfusion injury in the hearts of transgenic mice with a tamoxifen-regulated form of ATF6. Circ Res 2006;98:1186–93.
[27] Thuerauf DJ, Marcinko M, Gude N, Rubio M, Sussman MA, Glembotski CC. Activation of the unfolded protein response in infarcted mouse heart and hypoxic cultured cardiac myocytes. Circ Res 2006;99:275–82.
[28] Shintani-Ishida K, Nakajima M, Uemura K, Yoshida K. Ischemic preconditioning protects cardiomyocytes against ischemic injury by inducing GRP78. Biochem Biophys Res Commun 2006;345:1600–5.
[29] Luo S, Mao C, Lee B, Lee AS. GRP78/BiP is required for cell proliferation and protecting the inner cell mass from apoptosis during early mouse embryonic development. Mol Cell Biol 2006;26:5688–97.
[30] Reimold AM, Etkin A, Clauss I, Perkins A, Friend DS, Zhang J, et al. An essential role in liver development for transcription factor XBP-1. Genes Dev 2000;14:152–7.